Astron. Astrophys. 216, 44–61 (1989)

ASTRONOMY AND ASTROPHYSICS

Physical parameters of stars in the Scorpio-Centaurus OB association ★

E. J. de Geus [1,2], P. T. de Zeeuw [3], and J. Lub [1,4,★★]

[1] Sterrewacht Leiden, Postbus 9513, NL-2300 RA Leiden, The Netherlands
[2] Astronomy Department, University of Maryland, College Park, MD 20742, USA
[3] Institute for Advanced Study, Princeton, USA
[4] Observatorio del Roque de los Muchachos, La Palma, Spain

Summary. Walraven photometry is presented of established and probable members of the Scorpio-Centaurus OB association. For each star effective temperature and surface gravity are derived using Kurucz atmosphere models. From the Straižys and Kuriliene tables, absolute magnitudes are calculated. Distance moduli and visual extinctions are determined for all stars. From a comparison of the HR-diagrams of the stars in each subgroup with theoretical isochrones, the ages of the three subgroups are derived. The distances to the three subgroups are shown to be different; there is a general trend (also within each subgroup) for the distances to be larger at higher galactic longitudes. The visual extinction in the youngest subgroup Upper-Scorpius is well correlated with the IRAS 100 μm map. The distance towards the Ophiuchus dark clouds is found to be 125 pc, based on the photometric distances to the stars. Most of the early-type stars in Upper-Scorpius are located at the far side of the dark clouds.

Key words: clusters: associations – distances – photometry – stars: Hertzsprung-Russell diagram

1. Introduction

Since the work of Ambartsumian and Blaauw (see the review by Blaauw, 1964, and the references therein), OB associations have been in the focus of astronomical interest. The study of the stellar content of nearby OB associations is important for understanding starformation processes (e.g. Elmegreen and Lada, 1977), the nature and origin of the initial mass function, and the spatial distribution of high- and low-mass starformation during the evolution of a giant molecular cloud (e.g. Mathieu, 1986). For example, recent speculation that high- and low-mass stars form by different processes (e.g. Larson, 1986) can be tested directly by studying the mass functions of OB associations over as large a mass-interval as possible. However, a serious problem in these investigations is the lack of knowledge of reliable membership from proper-motion studies, even for the nearby OB associations. In most cases no main-sequence members of spectral type later than B 5 are known. The HIPPARCOS astrometric measurements of the nearby OB associations, as proposed by the SPECTER consortium at Leiden Observatory, are meant to remedy this situation. Results from HIPPARCOS are anticipated in 1992/1993.

Scorpio-Centaurus (or Sco OB 2) is the OB association nearest to the Sun, and is therefore very well suited to study the details of the interaction of the early-type stars with the interstellar medium. It consists of three well known subgroups: Upper-Scorpius, Upper-Centaurus Lupus and Lower-Centaurus Crux (Blaauw, 1964). Proper motion studies of this association by Blaauw (1946), Bertiau (1958) and Jones (1970) have established membership for stars with spectral types down to B 9 in Upper-Scorpius and to B 5 in Upper-Centaurus Lupus and Lower-Centaurus Crux, and have provided distances based on the convergent point method.

Photometric studies of Sco-Cen as a whole were made by Gutierrez-Moreno and Moreno (1968) and Glaspey (1971), and of Upper-Scorpius in particular by Hardie and Crawford (1961) and Garrison (1967). Our photometric study contains a larger number of stars than the previous studies, and it uses the latest calibrations of the absolute magnitude scale (Straižys and Kuriliene, 1981). The resulting distance estimates are therefore expected to be of higher accuracy. The comparison of the HR diagrams for the stars with recent models of stellar evolution allow an accurate determination of the relative and absolute ages of the subgroups.

The present paper deals with the photometric observations and the derivation of physical parameters of the stellar content of Sco OB 2. We define a large sample of stars, for which we obtained homogeneous photometric data with the Dutch 91-cm telescope on La Silla (see Sect. 2). In Sect. 3, several physical parameters, such as $\log T_{\mathrm{eff}}$, $\log g$, M_V, M_{bol}, $\log L/L_{\odot}$, A_V and the distance modulus, are derived from the photometry. In Sect. 4 HR-diagrams are constructed for the established member stars, the locations of several individual stars are discussed, and ages are derived for the three subgroups through isochrone fitting. The distance to the association is determined in Sect. 5 using the photometric distances to the established members. For all stars we will indicate the probability of membership on the basis of the distances of the separate stars compared to the mean of the subgroup. We also discuss the relation between the stars in Upper-Scorpius and the dark clouds in Ophiuchus. The distance to the dark clouds is determined from the A_V vs. distance modulus diagram of the stars in this subgroup.

This paper is the first of a series in which we will present and discuss observations of both the stars and the interstellar matter of the Upper-Scorpius/Ophiuchus region, and in which we will

---

Send offprint requests to: E.J. de Geus (USA address)

★ Based on *VBLUW* Photometry obtained with the 91-cm Dutch Telescope at ESO, La Silla

★★ On leave from Sterrewacht Leiden

present a model describing the present state of the aggregate of gas and stars from the perspective of an ongoing interaction.

2. Observations

2.1. Programme stars

The stars studied in this article are established or probable members of the Scorpio-Centaurus OB association. Reliable membership determinations from proper motion studies of stars of spectral type earlier than B 5 were made by Blaauw (1946) for the whole association. Bertiau (1958) added a number of fainter stars to the list of members of the Upper-Scorpius subgroup, also based on proper motions. For Upper-Scorpius therefore members are known down to B 9, but for the other two subgroups membership is only determined down to B 5. The total of proper-motion-members is 106, including the runaway star ζ Oph (Blaauw, 1961). The rest of the stars in our programme were taken from the CSI catalogue (Jung and Bischoff, 1971) with the restrictions that the spectral type is O or B, and of course that the coordinates are within the boundaries defined by Blaauw (1964). An additional 32 A 0-F 2 stars in a small region in Upper Scorpius, from a photometric study by Garrison (1967), were included. This results in a total of 309 stars in our programme. Photometry has been obtained for a much larger number of stars including later spectral types (de Geus et al., 1988). However the accuracy of those measurements is relatively low, so that they were not included in the present study.

When determining general properties of a subgroup or the whole association, we will restrict ourselves to the proper-motion members only.

The list of proper-motion member stars of course is by no means complete; the very existence of this study is due to that problem. Regarding the rest of the stars, we have to distinguish between different spectral types. The CSI catalogue is complete down to $m_V \approx 9^{\mathrm{m}}$ and is limited at $m_V \approx 12^{\mathrm{m}}$, so that the same limits hold for the early-type stars in our programme. The A and F stars of the photometric study by Garrison (1967) are located in a small area of Upper-Scorpius, with magnitude limit $m_V \approx 10\overset{\mathrm{m}}{.}5$.

The relatively low completeness limit of the sample will have important consequences for our study of the Upper-Scorpius region, where high values of the visual extinction are found.

2.2. Photometric system

The Walraven photometer mounted on the Dutch 91-cm telescope at ESO La Silla (Lub, 1979) was used for this study. The data were obtained in several observing sessions during the months of April to August in the years 1983 to 1987. The photometric system measures five bands simultaneously: V, B, L, U, and W. The properties of the passbands are given in Table 1 (from de Ruiter and Lub, 1985). More detailed information on the telescope and the photometric system can be found in Lub and Pel (1977).

Four independent colour indices can be obtained from the five bands: $(V-B)$, $(B-U)$, $(U-W)$, and $(B-L)$. For early-type stars $(V-B)$ measures the reddening, $(B-U)$ covers the Balmer jump and therefore measures the effective temperature, and both $(U-W)$ and $(B-L)$ are indicators of the surface gravity. The Walraven colours are defined in units of log (intensity). So unless another unit is specifically mentioned, we will use log (intensity) throughout this article. The conversion to units of magnitude is obtained by multiplying by -2.5.

2.3. Accuracy of the observations

The errors in the observations are mainly due to photon noise. The effect of this noise can be reduced by using sufficiently long integration times, depending on the brightness of the star. A study by de Ruiter and Lub (1985) showed that the 1% accuracy level, including the effect of subtracting the skybackground, for a $V_J = 13\overset{\mathrm{m}}{.}8$ star is reached after an integration of 64 s. Considering the magnitudes of the stars in our sample, the effects of photon statistics are hardly important. All stars were integrated long enough to ensure a good accuracy, and because the faintest stars are of 11$^{\mathrm{th}}$ magnitude, integration times were never longer than 1 min. Each star was observed at least 3 times on different nights, so the repeatability of the measurements is an indication of the accuracy of the observations. The mean RMS errors are: $\bar{\sigma}(V) = 0.0016$, $\bar{\sigma}(V-B) = 0.0008$, $\bar{\sigma}(B-U) = 0.0010$, $\bar{\sigma}(U-W) = 0.0009$, $\bar{\sigma}(B-L) = 0.0007$.

The results of the observations are listed in Table 2. The first three columns give the identifications of each star: column 1 is the HD number (HD), column 2 gives the running number in the SPECTER input catalogue for HIPPARCOS (HIPP), and column 3 gives the name. Column 4 gives the Walraven V-band. In columns 5–8 the Walraven colours are given: $(V-B)$, $(B-U)$, $(U-W)$ and $(B-L)$, respectively. Column 9 shows the number of measurements per star.

3. Derivation of physical parameters

The derivation of physical parameters from photometric data, involves a number of steps in which theoretical and empirical transformations are used. We will basically follow the procedure that was used by Brand and Wouterloot (1988, hereafter BW). In this section we give a schematic presentation of the steps necessary to determine effective temperature, surface gravity, visual extinction and the distance modulus. Further details can be found in

Table 1. Properties of the passbands in the Walraven system

	V	B	L	U	W
λ_{eff} (Å)	5441	4298	3837	3623	3235
Bandwidth (Å)	708	423	221	232	157
Cal. constant erg s cm^2 Å)	−11.172	−10.910	−10.818	−10.793	−10.673

Note: Numbers adopted from de Ruiter and Lub (1985)

Table 2a. Walraven colours for stars in Lower-Centaurus Crux

HD (1)	Hipp (2)	Name (3)	V (4)	(V − B) (5)	(B − U) (6)	(U − W) (7)	(B − L) (8)	# (9)
99264	7341		0.5258	0.0296	0.1158	0.0356	0.0436	5
99556	6775	θ^2Cru	0.6439	−0.0187	0.1398	0.0323	0.0292	6
100929	6777		0.4206	−0.0288	0.1088	0.0162	0.0247	4
102776	6967		1.0276	−0.0530	0.1157	0.0064	0.0294	5
103079	7022		0.7996	−0.0446	0.1330	0.0062	0.0518	5
103884	6855		0.5263	−0.0567	0.0973	−0.0018	0.0323	7
104841	6913		0.8650	−0.0274	0.1074	0.0119	0.0320	5
104878	7188		0.6178	−0.0010	0.3233	0.0665	0.1288	5
105382	5992		0.9577	−0.0530	0.0725	−0.0120	0.0087	8
105383	6111		0.2067	−0.0186	0.3244	0.0621	0.1169	5
105416	5853		0.6195	−0.0034	0.4218	0.1123	0.1267	4
105435	6113	δCen	1.7216	−0.0443	−0.0346	0.0021	−0.0128	7
105580	6724		−0.1024	−0.0143	0.1504	0.0267	0.0516	5
105937	6238	ρCen	1.1717	−0.0580	0.1114	−0.0024	0.0377	6
106490	6663	δCru	1.6414	−0.0799	−0.0182	−0.0309	−0.0216	6
107696	6557		0.6021	−0.0355	0.2190	0.0395	0.0716	5
108257	6133		0.8288	−0.0533	0.1077	0.0045	0.0313	7
109026	7343	γMus	1.2172	−0.0539	0.1169	0.0110	0.0344	6
109668	7237	αMus	1.6804	−0.0744	0.0136	−0.0237	−0.0056	7
110335	6732		0.7684	−0.0013	0.2107	0.0760	0.0509	5
110879	7194	βMus	1.5379	−0.0656	0.0529	−0.0133	0.0138	5
110956	6512		0.9040	−0.0557	0.0978	−0.0011	0.0334	6
111123	6733	βCru	2.2589	−0.0819	−0.0570	−0.0381	−0.0418	3
111613	6737		0.4618	0.1746	0.3283	0.2456	0.0975	6
112078	6682	λCru	0.9083	−0.0530	0.1180	0.0072	0.0339	7
112091	6570	μ^2Cru	0.6860	−0.0369	0.1488	0.0241	0.0560	6
112092	6569	μ^1Cru	1.1499	−0.0647	0.0445	−0.0138	0.0099	6
113314	5940	ξ^1Cen	0.8191	0.0087	0.4340	0.1054	0.1691	7
113703	5865		0.8728	−0.0515	0.1302	0.0048	0.0467	7
113791	6056	ξ^2Cen	1.0467	−0.0675	0.0318	−0.0193	0.0055	7
115823	6369		0.5692	−0.0451	0.1671	0.0193	0.0600	7
115846	7149		−0.0606	−0.0078	0.1466	0.0218	0.0568	5
116072	6823		0.2747	0.0118	0.1145	0.0333	0.0375	8
116087	6822		0.9461	−0.0491	0.1195	0.0037	0.0418	6
116226	5870		0.2104	−0.0202	0.2002	0.0557	0.0437	5
118716	6373	ϵCen	1.8397	−0.0786	−0.0287	−0.0312	−0.0282	6
118978	6698		0.6027	−0.0043	0.3103	0.0864	0.0832	5
120908	6378		0.4047	0.0123	0.2019	0.0586	0.0626	6
123335	6706		0.2169	0.0280	0.1519	0.0451	0.0605	6
124182	7105		−0.0237	0.0028	0.1304	0.0342	0.0397	6

BW. The errors introduced in the different steps are discussed at the end of each section. The procedure we used to determine the errors in the final result is to take the specific combination of input parameters (and their errors) that will result in the maximum deviation in the end result. The probable error in the end result is then estimated as half this maximum error.

3.1. *Reddening-free colours*

In order to avoid having to solve for reddening when determining $\log T_{\rm eff}$ and $\log g$, reddening-free colours (RFC's) were defined in the same way as the Q-colours in the UBV-system (Lub and Pel, 1977). The three reddening-free parameters in the Walraven system are defined as:

$$\begin{aligned} [B-U] &= (B-U) - 0.61\ (V-B)\,, \\ [U-W] &= (U-W) - 0.45\ (V-B)\,, \\ [B-L] &= (B-L) - 0.39\ (V-B)\,. \end{aligned} \tag{1}$$

The colour $(V-B)$ basically only measures the reddening, therefore the reddening-free colours still have the same physical meaning as the principal colour they are derived from. So $[B-U]$ is an indicator of $\log T_{\rm eff}$, and each of $[U-W]$ and $[B-L]$ determine $\log g$.

The errors in the reddening-free colours have two independent sources. The observational errors in the colours will influence the errors in the RFC's in a straightforward way. The coefficients in Eq. (1) are the slopes of the reddening lines in the corresponding colour-colour diagrams, and are therefore based on the value of total to selective extinction: $R = 3.2 \pm 0.2$, (an average value of several studies: Harris, 1973; Hackwell and Gehrz, 1974; Schultz and Weimar, 1975; Barlow and Cohen, 1977; Sneden et al., 1978). This value may differ from one region to the other, and especially the region around ϱ Oph is known to have a deviating R (Gutierrez-Moreno et al., 1968; Whittet, 1974). In order to obtain an internally consistent set of results, we will use the conventional value of R throughout this article. This may lead to errors, especially for highly extinguished stars (e.g. the results for HD 147889 cannot be trusted). However, most of the stars studied here have small visual extinctions, and hence errors in the value of R have a negligible effect.

3.2. *Effective temperature and gravity; reddening corrected colours*

In order to determine the effective temperature and surface gravity of a star from its reddening-free colours, we used a grid of theoretical colours for a wide range of $T_{\rm eff}$ and $\log g$. The Kurucz (1979) atmosphere models (stellar spectral energy distributions for different temperatures, gravities and abundances) were folded with the Walraven passbands, in order to obtain this grid (henceforth: "Kurucz grid"). Absolute calibration of the Kurucz grid is done by comparing the colours of stars having either a known energy distribution or known $T_{\rm eff}$ and $\log g$, with the theoretical colours. As was shown by BW, the Kurucz models do not give an adequate description of the atmospheres of both cool ($T_{\rm eff} < 8000$ K) and very hot ($T_{\rm eff} > 30000$ K) stars. As a result the grids in the two-colour diagrams should not be trusted for these stars. Few stars in our programme fall in the cool part of the grid, and we have ignored them. Because of their importance in this study, hot stars which have a colour outside the Kurucz grid are given the temperature and gravity of the point in the grid closest to that of the star. Great care was taken that these hot stars would not introduce spurious effects in the age or distance determination.

A different chemical composition obviously affects the theoretical colours. The Kurucz models were calculated for different values of the metal-abundance, however for the range of physical parameters of interest here the influence on the theoretical atmospheres is negligible. Much more important is the effect upon the interior structure of the star, i.e. upon the mass-luminosity relation. For studies on young associations at greater distances from the solar circle than the association studied here, this effect obviously has to be taken into account. Chemically peculiar stars are known to have a distorted spectral energy distribution. In the case of the Scorpio-Centaurus stars such peculiarities are known beforehand from available spectroscopic studies. These objects have *not* been included in the final distance and age determination. It is of considerable interest to study the effect of chemical peculiarities in a systematic way, however we prefer to refer this discussion to the presentation of the complete set of *VBLUW* data taken for the SPECTER programme and the HIPPARCOS input catalogue.

The availability of three reddening-free parameters enables us to construct two independent reddening-free colour-diagrams (RFD): $[B-U]$ vs. $[U-W]$ and $[B-U]$ vs. $[B-L]$. Due to uncertainties in the calibration of the grid in the $[B-U]$ vs. $[U-W]$ plane (the clearly defined empirical main-sequence lies outside the grid), we decided to use only the $[B-U]$ vs. $[B-L]$ diagram. Any further reference to the reddening-free colour-diagram will mean the latter. Figure 1 shows the Kurucz grid in

Table 2b. Walraven colours for stars in Upper-Centaurus Lupus

HD (1)	Hipp (2)	Name (3)	V (4)	(V − B) (5)	(B − U) (6)	(U − W) (7)	(B − L) (8)	# (9)
118335	4389		−0.3068	0.0129	0.4157	0.0976	0.1818	5
119103	4834		−0.0995	−0.0185	0.3496	0.0855	0.1000	4
119221	4835		−0.1580	0.0692	0.4308	0.1298	0.2116	4
119338	4447		−0.8163	−0.0384	0.1591	0.0198	0.0565	7
119361	4731		0.3674	−0.0250	0.2744	0.0680	0.0705	5
119430	4837		−0.0841	−0.0044	0.4220	0.1116	0.1301	3
119674	4344		−0.8629	0.1300	0.4579	0.1811	0.2328	8
120307	4736	νCen	1.3893	−0.0780	−0.0077	−0.0298	−0.0151	7
120324	4737	μCen	1.3711	−0.0736	0.0255	−0.0183	−0.0033	6
120487	4637		−0.8499	0.1032	0.4113	0.1532	0.2127	6
120640	5248		0.4516	−0.0537	0.0504	−0.0104	0.0115	4
120709	4196	3 Cen	0.9595	−0.0500	0.0814	0.0008	0.0270	8
120710	4195	3 Cen	0.3856	−0.0171	0.3117	0.0551	0.1196	6
120908	6378		0.4047	0.0123	0.2019	0.0586	0.0626	6
120955	4164	4 Cen	0.8566	−0.0486	0.1456	0.0214	0.0340	5
120959	4510		−0.7432	0.0550	0.4772	0.1547	0.1961	5
120960	4744		−0.3894	0.1380	0.3730	0.1651	0.2029	5
121057	5421		−0.1235	0.0728	0.4579	0.1428	0.2177	4
121190	5668		0.4909	−0.0257	0.2750	0.0460	0.1069	4
121226	5252		−0.2236	0.0349	0.4536	0.1220	0.1941	4
121292	5347		−0.8487	−0.0121	0.2718	0.0538	0.0964	5
121399	4511		−0.1285	0.1640	0.4809	0.1610	0.2171	6
121528	4641		−0.9289	0.1438	0.4216	0.1929	0.2172	6
121743	4750	φCen	1.2289	−0.0770	0.0121	−0.0250	−0.0057	6
121790	5031	υ[1]Cen	1.2132	−0.0752	0.0237	−0.0221	0.0016	6
121983	4201		−0.4811	−0.0311	0.0479	0.0169	0.0011	6
122109	4353		−0.4552	0.0127	0.4468	0.1190	0.1656	4
122159	5354		−0.6763	−0.0036	0.2805	0.0623	0.0973	6
122324	5789		−0.8812	0.1684	0.0595	0.0873	0.0417	7
122449	5263		−0.4936	−0.0220	0.2056	0.0444	0.0586	6
122479	5678		−0.1909	−0.0175	0.1045	0.0121	0.0417	4
122664	4394		−0.5855	0.0897	0.4283	0.1524	0.2082	4
122705	5521		−0.3046	0.0508	0.4347	0.1214	0.2096	5
122756	4651		−0.7205	0.1587	0.3298	0.1677	0.1945	7
122757	4652		−0.7055	0.0495	0.4511	0.1354	0.2006	6
122925	5752		−0.4815	−0.0027	0.2215	0.0532	0.0735	5
122980	4654	χCen	1.0149	−0.0721	0.0379	−0.0221	0.0083	3
123021	4655		−0.5872	0.1058	0.4014	0.1572	0.2015	5
123130	5728		−0.7317	0.0175	0.2495	0.0710	0.0880	6
123291	4939		−0.5421	0.0076	0.3838	0.0927	0.1342	5
123344	4304		−0.1893	0.0122	0.4070	0.0994	0.1624	6
123431	4754		−0.7384	0.0013	0.4100	0.0910	0.1597	5
123635	4941		−1.9379	0.2098	0.3759	0.1953	0.2156	2
123635	4942		−0.3424	−0.0036	0.2365	0.0682	0.0683	7
123664	5151		−0.3037	0.0406	0.4923	0.1458	0.1823	6
124228	4585		−0.3928	0.0696	0.4702	0.1524	0.2022	6
124254	5155		−0.2245	0.0894	0.4223	0.1493	0.2037	4
124367	5802		0.7553	−0.0103	0.0804	0.0331	0.0363	4
124504	4170		−0.4966	0.0978	0.4364	0.1532	0.2146	7
125238	5157	ιLup	1.3366	−0.0653	0.0667	−0.0076	0.0147	4
125253	5158		−0.0853	0.0314	0.4453	0.1101	0.1991	5
125509	4311		−0.3288	−0.0093	0.3890	0.0908	0.1296	5
125541	4763		−0.8012	0.1283	0.3751	0.1630	0.2039	5
125718	4764		−0.9493	0.0859	0.4571	0.1539	0.2154	6
125721	5367		0.3184	−0.0385	−0.0306	−0.0141	−0.0249	5
125823	4519		0.9896	−0.0694	0.0479	−0.0158	0.0121	7
125937	5161		−0.4896	0.1004	0.4263	0.1543	0.2069	5
126062	5272		−0.2284	0.0263	0.4276	0.1044	0.1981	5
126194	4402		0.0731	0.0474	0.3978	0.1094	0.1907	3
126341	5051	τ[1]Lup	0.9288	−0.0504	0.0243	−0.0109	−0.0014	4
126476	4589		−0.4778	0.0729	0.4519	0.1474	0.2135	5
126561	5166		−0.1352	0.0016	0.4015	0.0822	0.1698	4
126981	5055		0.5513	−0.0299	0.2983	0.0624	0.0889	4
127716	4771		0.1141	0.0281	0.5042	0.1668	0.1619	4
127717	4770		−0.8673	0.1336	0.3949	0.1697	0.2033	5
127778	4772		−1.1913	0.1833	0.3949	0.2035	0.2189	5
127879	4951		−0.3874	0.1040	0.4086	0.1537	0.2051	5
127972	4773	ηCen	1.7797	−0.0720	0.0338	−0.0086	−0.0148	6
128066	4669		−0.8050	0.1401	0.3582	0.1657	0.1924	5
128224	4407		−0.3252	−0.0240	0.1927	0.0442	0.0580	5
128344	5372		0.0894	−0.0038	0.2924	0.0708	0.0879	4
128532	4321		0.0401	0.0668	0.4605	0.1421	0.2100	4
128788	4670		−0.5689	0.0783	0.4244	0.1378	0.2126	5
128819	4671		0.0954	−0.0250	0.2904	0.0530	0.1018	4
128855	4672		−0.1911	0.0260	0.4724	0.1464	0.1607	5
129056	5287	αLup	1.8331	−0.0724	−0.0099	−0.0237	−0.0240	6
129116	4468		1.1554	−0.0633	0.0702	−0.0092	0.0216	6
129791	5064		−0.0127	0.0191	0.4027	0.0982	0.1659	5
130163	4600		−0.0128	0.0096	0.4299	0.1090	0.1635	4
130388	4367		−0.3031	0.0777	0.4538	0.1468	0.2114	5
130807	4960	οLup	1.0214	−0.0548	0.1111	0.0109	0.0367	6
131120	4476		0.7457	−0.0588	0.0667	−0.0054	0.0209	5
131399	4280		−0.0696	0.0428	0.4315	0.1117	0.2037	4
131460	4369		−0.8428	0.1271	0.4268	0.1652	0.2166	6
131461	4370		−0.1408	0.0281	0.4225	0.0978	0.1896	5
131503	4973		−0.4467	0.0981	0.4570	0.1648	0.2151	5
131518	4974		−0.9019	0.1235	0.4316	0.1683	0.2161	6
131752	4538		0.2094	0.0260	0.4057	0.1027	0.1694	4
131777	4780		−0.5065	0.0310	0.4353	0.1133	0.1920	6
131901	4231		−0.1260	0.0396	0.4522	0.1215	0.1847	4
132058	4874	βLup	1.6819	−0.0782	−0.0079	−0.0273	−0.0193	5
132080	4781		−1.1301	0.1253	0.4322	0.1710	0.2226	7
132094	4422		−0.1528	−0.0106	0.3635	0.0756	0.1322	3
132200	4782	κCen	1.5007	−0.0722	0.0351	−0.0185	0.0006	6
132761	4185		−0.3451	0.0965	0.4323	0.1497	0.2131	6
132851	4051	60 Hya	0.4182	0.0705	0.4733	0.1556	0.2092	4
132955	4237		0.5776	−0.0421	0.1158	0.0052	0.0423	3
133574	4331		−0.7349	0.1348	0.3905	0.1647	0.2057	5
133750	4238		−0.1191	0.0227	0.4357	0.1021	0.1810	4
133937	4886		0.4242	−0.0408	0.1929	0.0286	0.0628	4
133955	5071	λLup	1.1316	−0.0610	0.0827	−0.0078	0.0256	5
134055	4541		−0.1448	0.1072	0.4103	0.1503	0.2132	4
134518	4377		−0.9592	0.1323	0.4489	0.1742	0.2270	5
134685	4334		−0.3178	0.0568	0.4442	0.1225	0.1885	5
134687	5075		0.8243	−0.0633	0.0791	−0.0080	0.0248	5
134930	4978		−0.1932	0.0756	0.4285	0.1340	0.2113	5
134950	4380		−0.5784	0.1063	0.4796	0.1622	0.2268	5
134990	4547		−0.0731	0.0485	0.4457	0.1335	0.1914	4
135454	4793		0.0491	−0.0116	0.3730	0.0816	0.1386	5
135814	4699		−0.7356	0.1293	0.3939	0.1720	0.2085	6
135877	4701		−0.7428	0.0841	0.4736	0.1727	0.1946	5
136013	4287		−0.3533	0.0348	0.4342	0.1035	0.1906	5
136164	4337		−0.3640	0.0779	0.4307	0.1377	0.2065	5
136298	4704	δLup	1.4644	−0.0788	−0.0130	−0.0287	−0.0197	5
136334	4705		0.2730	0.0279	0.4483	0.1159	0.1920	5
136482	4494		0.0941	−0.0243	0.3131	0.0613	0.1094	4
136483	4706		−0.8171	0.1926	0.4426	0.2428	0.2177	4
136504	5078	εLup	1.4030	−0.0689	0.0475	−0.0142	0.0097	4
136664	4438	φ[2]Lup	0.9379	−0.0562	0.1013	−0.0007	0.0347	6
136961	4385		0.0533	0.0273	0.4487	0.1240	0.1910	4
137169	4709		−0.8381	0.0642	0.4829	0.1564	0.2032	5
137193	4613		−0.1985	0.0051	0.3046	0.0995	0.1162	3
137432	4441		0.5684	−0.0546	0.1257	0.0077	0.0432	5
137785	4558		0.1737	0.1410	0.3661	0.1712	0.1954	4
137957	5081		−0.2284	0.0275	0.4587	0.1256	0.1754	4
138285	4502		−0.2464	0.0105	0.4100	0.0897	0.1817	5
138564	4563		0.2050	−0.0103	0.3744	0.0680	0.1495	4
138690	4714	γLup	1.6444	−0.0752	0.0133	−0.0229	−0.0076	5
138769	5085		0.9341	−0.0675	0.0755	−0.0101	0.0225	5
138940	4716		−0.2966	−0.0141	0.3591	0.0739	0.1275	4
139048	4565		−0.8925	0.1431	0.4063	0.1775	0.2104	6
139233	4566		0.1198	−0.0256	0.3248	0.0579	0.1176	4
139524	5002		−0.4677	0.0074	0.3416	0.0828	0.1102	6
140008	3862	ψ[2]Lup	0.8592	−0.0520	0.1447	0.0098	0.0539	5
140602	5005		−0.5518	0.0688	0.4376	0.1350	0.2140	6
142201	4626		−1.4503	0.0920	0.4325	0.1473	0.1748	11
143118	3970	ηLup	1.3842	−0.0807	−0.0032	−0.0263	−0.0153	6
143699	3971		0.7948	−0.0525	0.1214	0.0116	0.0421	4
144294	3928	θLup	1.0663	−0.0657	0.0681	−0.0096	0.0184	4

Table 2c. Walraven colours for stars in Upper Scorpius

HD (1)	Hipp (2)	Name (3)	V (4)	(V − B) (5)	(B − U) (6)	(U − W) (7)	(B − L) (8)	# (9)
138138	3830		0.0008	0.0697	0.4182	0.1335	0.2101	4
139094	3394		−0.2054	0.0372	0.2617	0.0704	0.1065	4
139365	3622		1.2900	−0.0638	0.0750	−0.0085	0.0236	5
139486	2945		−0.2990	0.0164	0.3785	0.0803	0.1534	4
140475	3865		−0.3346	0.0415	0.4288	0.1129	0.2067	6
140817	3890		0.0183	0.0085	0.3615	0.0791	0.1520	3
140958	3947		−0.4764	0.0886	0.4092	0.1444	0.2050	5
141180	3492		−0.5566	−0.0054	0.2964	0.0606	0.1064	6
141404	3000		−0.3335	0.0558	0.4538	0.1413	0.1483	5
141556	3835	χLup	1.1645	−0.0173	0.3615	0.0829	0.1274	4
141637	3321	1 Sco	0.8975	−0.0162	0.0481	0.0013	0.0205	3
141774	3001		−0.3287	0.0360	0.3724	0.0938	0.1378	6
141905	3986		−0.5778	0.0956	0.4932	0.1637	0.2201	6
141939	3401		−0.5456	0.0865	0.4569	0.1440	0.2253	5
142097	3038		−0.6174	0.1569	0.4740	0.1731	0.2436	5
142114	3247	2 Sco	0.9125	−0.0234	0.0894	0.0057	0.0362	4
142165	3248		0.6007	0.0005	0.2052	0.0398	0.0797	4
142184	3169		0.5921	−0.0046	0.1026	0.0231	0.0451	5
142250	3402		0.2931	−0.0238	0.1949	0.0309	0.0757	5
142315	3095		0.0082	0.0181	0.3132	0.0690	0.1208	4
142378	2911	47 Lib	0.3725	0.0001	0.1480	0.0228	0.0652	3
142431	4000		−0.0732	0.0455	0.4434	0.1288	0.2006	4
142669	3572	ρSco	1.2020	−0.0708	0.0229	−0.0194	0.0000	6
142805	3043		−0.1061	0.0678	0.4539	0.1395	0.1543	4
142883	3004		0.4190	0.0151	0.1595	0.0307	0.0744	3
142884	3173		0.0438	0.0116	0.1735	0.0420	0.0715	4
142983	2809	48 Lib	0.7904	−0.0239	0.2148	0.0577	0.0367	6
142990	3252		0.5803	−0.0307	0.0918	0.0109	0.0349	4
143018	3330	πSco	1.5979	−0.0614	−0.0254	−0.0266	−0.0192	4
143275	3098	δSco	1.8253	−0.0355	−0.0320	−0.0162	−0.0198	4
143567	3045		−0.1284	0.0409	0.3620	0.0873	0.1463	3
143600	3099		−0.1805	0.0395	0.3828	0.0980	0.1497	4
143692	3100		−0.4391	0.0863	0.4667	0.1524	0.2130	4
144217	2956	β^1Sco	1.6645	−0.0214	−0.0167	−0.0122	−0.0132	11
144218	2957	β^2Sco	0.7799	−0.0012	0.0743	0.0107	0.0333	5
144334	3180		0.3848	−0.0247	0.1354	0.0236	0.0501	5
144470	3010	ω^1Sco	1.1738	−0.0020	0.0027	−0.0007	0.0008	3
144661	3254		0.2225	−0.0153	0.1542	0.0308	0.0596	4
144844	3184		0.4028	0.0102	0.2517	0.0512	0.1067	4
144941	3418		−1.3024	0.0196	0.0314	0.0566	0.0205	4
145102	3419		0.1117	0.0304	0.3361	0.0893	0.1170	3
145353	3420		−0.0272	0.0545	0.3790	0.0996	0.1419	4
145468	3102		−0.5404	0.1362	0.4720	0.1683	0.2300	7
145482	3508		0.9217	−0.0566	0.0497	−0.0100	0.0153	3
145483	3582		0.4835	0.0019	0.3316	0.0718	0.1305	4
145501	2959	νSco^C	0.2399	0.0534	0.2175	0.0670	0.0968	5
145502	2960	νSco^A	1.1504	0.0245	0.0779	0.0170	0.0404	4
145519	2916		−0.4446	0.1017	0.3997	0.1170	0.1649	5
145554	2961		−0.3046	0.0615	0.3683	0.0911	0.1509	5
145631	2962		−0.2844	0.0609	0.3917	0.1027	0.1558	5
145792	3259		0.1913	0.0179	0.1797	0.0361	0.0798	3
145793	3512		−0.4256	0.0979	0.4448	0.1437	0.2188	3
146001	3341		0.3273	0.0194	0.2222	0.0498	0.0901	4
146029	3104		−0.2002	0.0349	0.3908	0.0937	0.1473	5
146284	3186		0.0725	0.0670	0.3353	0.1025	0.1193	5
146285	3260		−0.4165	0.0937	0.3468	0.1002	0.1490	5
146332	3646		−0.2977	0.0871	0.2222	0.0945	0.0828	5
146416	3016		0.1124	0.0072	0.3405	0.0732	0.1267	4
146606	3513		−0.0747	−0.0029	0.3831	0.0805	0.1561	3
146706	3107		−0.2582	0.0502	0.3740	0.0985	0.1441	4
146899	3425		−1.3503	0.2659	0.5354	0.2348	0.2676	9
146998	3343		−1.0765	0.2682	0.4968	0.1984	0.2773	7
147009	2964		−0.4758	0.1202	0.4794	0.1409	0.2172	5
147010	2965		−0.2019	0.0654	0.2470	0.1130	0.1043	5
147012	3345		−1.1684	0.2062	0.4767	0.1700	0.2112	10
147013	3344		−0.8859	0.1725	0.5074	0.1666	0.2387	5
147084	3188	o Sco	0.9242	0.3532	0.7280	0.4000	0.2632	3
147105	3346		−0.7790	0.2051	0.5124	0.2065	0.2311	6
147165	3347	σSco	1.5919	0.0645	0.0335	0.0241	0.0194	4
147196	3189		−0.0659	0.0697	0.3351	0.0998	0.1240	5
147283	3264		−1.3734	0.3522	0.6341	0.2622	0.3306	4
147343	3265		−0.9936	0.2756	0.5680	0.2200	0.2729	4
147384	3266		−0.6902	0.1617	0.4952	0.1595	0.2219	6
147432	3110		−0.2655	0.1075	0.4427	0.1392	0.2218	4
147592	3349		−0.8180	0.1234	0.4809	0.1422	0.2337	6
147648	3351		−1.0347	0.3163	0.4504	0.2033	0.2140	8
147649	3350		−1.1010	0.1849	0.4951	0.1763	0.2516	6
147701	3267		−0.6001	0.2364	0.3139	0.1407	0.1638	5
147702	3352		−0.9126	0.1890	0.5133	0.1805	0.2582	6
147703	3428		−0.2396	0.0709	0.4114	0.1085	0.1624	5
147809	3353		−0.6941	0.1671	0.5091	0.1617	0.2431	6
147888	3191		0.0483	0.1328	0.2021	0.0704	0.1023	6
147889	3268		−0.4246	0.3640	0.2225	0.1517	0.1339	7
147890	3653		−0.3145	0.0939	0.3483	0.1330	0.1204	3
147932	3194		−0.1623	0.1290	0.1956	0.0744	0.1006	4
147933	3192	ρOph^A	0.9170	0.1036	0.0901	0.0435	0.0435	2
147934	3193	ρOph^B	0.9050	0.0992	0.0944	0.0460	0.0569	1
147955	3430		−0.4831	0.1024	0.3992	0.1132	0.1749	7
148117	3432		−1.5051	0.1051	0.4258	0.1574	0.1848	7
148118	3431		−1.0375	0.1776	0.5337	0.1892	0.2508	6
148184	2921	χOph	1.0229	0.1313	−0.0034	0.0731	0.0342	4
148199	3654		−0.0580	0.0395	0.3146	0.0931	0.1158	4
148302	3434		−1.2488	0.2099	0.4830	0.2094	0.2457	6
148321	3355		−0.0419	0.0819	0.4350	0.1389	0.2129	5
148334	3435		−1.2246	0.0801	0.3562	0.0944	0.1449	7
148499	3516		−1.1843	0.1535	0.4654	0.1561	0.1746	4
148562	3270		−0.3811	0.0656	0.4432	0.1285	0.2133	5
148563	3438		−0.6906	0.0920	0.4668	0.1326	0.2193	4
148594	3517		−0.0092	0.0458	0.2818	0.0802	0.1008	3
148605	3272	22 Sco	0.8397	−0.0448	0.0617	−0.0062	0.0223	5
148624	3440		−1.3971	0.1678	0.5106	0.1926	0.2470	6
148703	3879		1.0584	−0.0572	0.0208	−0.0177	0.0023	4
148822	3443		−1.1077	0.1963	0.4241	0.1978	0.2291	5
148842	3444		−1.5054	0.1016	0.4810	0.1485	0.2120	7
148860	2897		−0.4637	0.0641	0.3907	0.1099	0.1511	5
149069	3445		−1.4463	0.0842	0.4645	0.1275	0.1924	4
149168	3446		−1.2137	0.0323	0.2413	0.0568	0.1029	5
149228	3359		−1.2502	0.1357	0.2852	0.1140	0.1250	6
149367	3447		−0.6579	0.0652	0.3505	0.0985	0.1336	5
149387	3718		−0.9308	0.0725	0.2400	0.0836	0.0932	4
149438	3519	τSco	1.6247	−0.0857	−0.0799	−0.0443	−0.0467	3
149464	3590		−0.6897	0.0715	0.3949	0.1087	0.1567	3
149757	84	ζOph	1.7248	0.0212	−0.0239	0.0150	−0.0104	3
149883	3448		−0.6274	0.0568	0.3909	0.1058	0.1462	5
150035	3521		−0.7238	0.1011	0.4774	0.1646	0.1919	3
150347	3591		−0.8425	0.0371	0.3674	0.1018	0.1282	5
150514	2969		−0.7083	0.0512	0.3077	0.1026	0.1009	7
151310	3061		−0.9968	0.0214	0.1149	0.0297	0.0462	5
151346	3196		−0.4205	0.1768	0.2911	0.1358	0.1269	8
151831	3453		−1.4539	0.0299	0.2828	0.0827	0.0981	4
151865	2975		−0.7871	0.0678	0.3129	0.0970	0.1268	6
151890	748	μ^1Sco	1.5540	−0.0691	0.0068	−0.0271	−0.0107	5
151985	750	μ^2Sco	1.3317	−0.0741	−0.0032	−0.0253	−0.0147	3
154481	3460		0.2460	−0.0095	0.2906	0.0886	0.0744	4
157056	3303	θOph	1.4492	−0.0728	0.0009	−0.0234	−0.0106	4

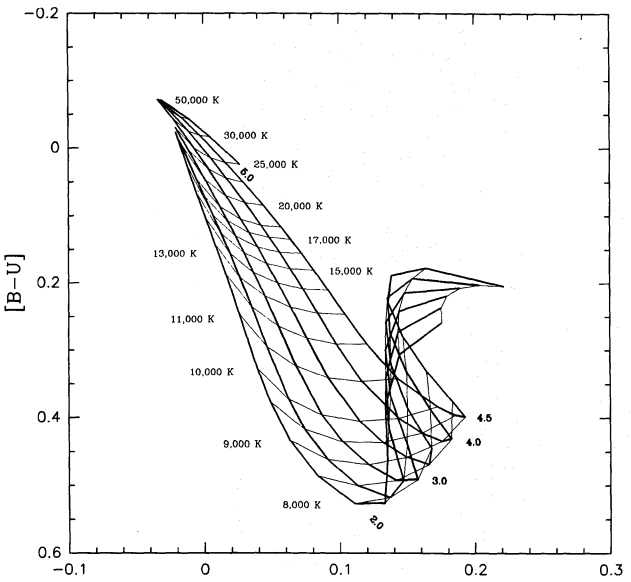

Fig. 1. Grid of log $T_{\rm eff}$ and log g in the reddening-free two-colour diagram of $[B-U]$ vs. $[B-L]$ (Kurucz grid). The thin drawn lines are lines of constant effective temperature, the thick drawn lines are lines of constant surface gravity. The values at the grid-lines are indicated

this diagram. log $T_{\rm eff}$ and log g can now be determined by two-dimensional linear interpolation in the grid.

Inversely, it is clear that we can use the same grid, but now in normal-colour space, to transform log $T_{\rm eff}$ and log g into the reddening corrected colours, i.e. the colours that the star of given effective temperature and surface gravity would have had in the absence of extinction. In practice only the reddening corrected $(V-B)$ is used further.

The errors in the derived log $T_{\rm eff}$ and log g will basically be due to the propagation of the errors in the original input-colours. From Fig. 1 it is clear that, because the grid gets narrower at higher $T_{\rm eff}$, the errors will be larger at higher $T_{\rm eff}$. From the calculated propagation of the errors we find that $\bar{\sigma}(\log T_{\rm eff}) \approx 0.015$ for log $T_{\rm eff} < 4.3$ and $\bar{\sigma}(\log T_{\rm eff}) \approx 0.03$ for log $T_{\rm eff} \geqq 4.3$. For log g we find that $\bar{\sigma}(\log g) \approx 0.1$ for log $T_{\rm eff} < 4.3$ and $\bar{\sigma}(\log g) \approx 0.25$ for log $T_{\rm eff} \geqq 4.3$.

3.3. Absolute magnitude; log $L/L_\odot$

From log $T_{\rm eff}$ and log g we can now determine the absolute visual magnitude and the absolute bolometric magnitude. Straižys and Kuriliene (1981) published tables with log $T_{\rm eff}$, log g, M_V, $M_{\rm bol}$, spectral type, and luminosity class, based on both observations and theoretical calculations. Figure 2 shows their coverage in log $T_{\rm eff}$, log g space. Two-dimensional linear interpolation is used to derive M_V and $M_{\rm bol}$. The luminosity is calculated from the bolometric magnitude using the relation:

$$\log \frac{L}{L_\odot} = -0.4\, M_{\rm bol} + 1.888 . \qquad (2)$$

The absolute magnitude of a star is very sensitive to both $T_{\rm eff}$ and log g, so that the errors in the derived temperature and gravity will cause large uncertainties in the values of M_V and $M_{\rm bol}$. Again we can calculate the propagation of the errors for each star. A plot of $\sigma(M_V)$ as a function of log $T_{\rm eff}$ shows that $\overline{\sigma(M_V)} \approx 0\overset{\rm m}{.}3$. This will of course result in errors of the same magnitude in the final distance modulus.

3.4. Colour excess, visual extinction and distance modulus

The colour excess in the Walraven system, $E_{(V-B)}$, is calculated from the observed colour $(V-B)$ and the reddening corrected colour $(V-B)_0$: $E_{(V-B)} = (V-B) - (V-B)_0$. In order to calculate the visual extinction in the Johnson *UBV*-system, we first have to calculate the colour excess in the Johnson system from that in the Walraven system, using the formula:

$$E_{(B-V)_{\rm J}} = 2.39 \times E_{(V-B)_{\rm W}} - 0.17 \times E^2_{(V-B)_{\rm W}} \qquad (3)$$

(Pel, 1987, private communication). From $A_V = R \times E_{(B-V)}$ and $R = 3.2 \pm 0.2$, A_V can then be calculated.

As a check on the derived values of A_V, we have taken published Strömgren *uvby* photometry from Mermilliod and

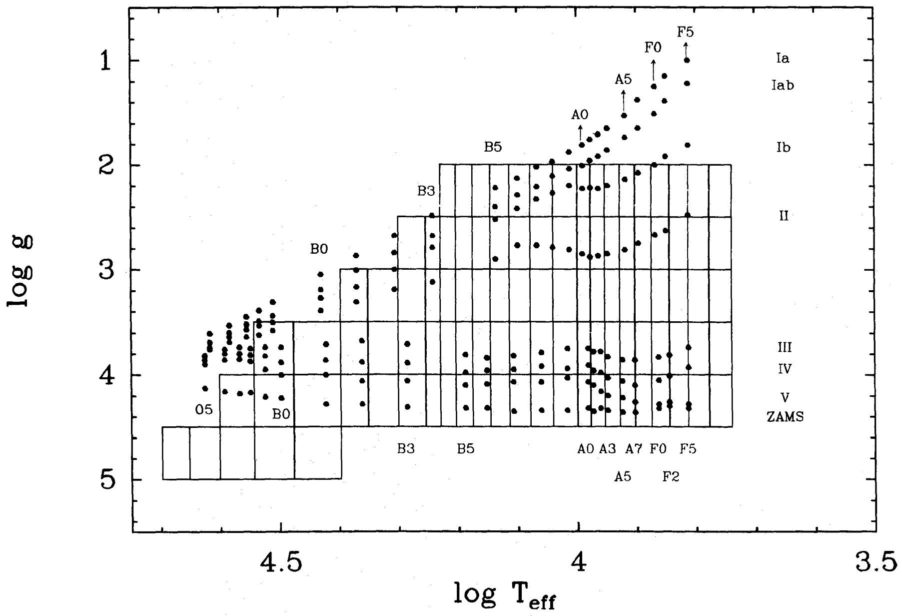

Fig. 2. Coverage in the (log $T_{\rm eff}$, log g) plane of the Straižys and Kuriliene grid (points) and the Kurucz grid (lines). For the Straižys and Kuriliene points the corresponding spectral type (vertical) and luminosity class (horizontal) are indicated. Note that especially for the earliest spectral types the two grids do not overlap

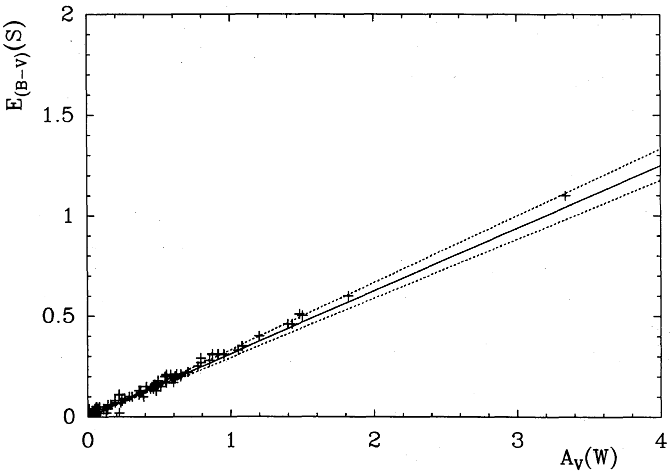

Fig. 3. Differential reddening $E_{(B-V)}$ calculated from Strömgren photometric data vs. the visual extinction calculated from the Walraven photometry. The line gives the standard ratio between A_V and $E_{(B-V)}$: $R=3.2$. The dashed lines give the upper and lower limits to R. The data all lie close to the line $R=3.2$, which indicates the validity of the procedure used in this study

Hauck (1980) for stars in our sample, and used the empirical calibration of Crawford (1978) to derive the visual extinction $E_{(b-y)}$. For a normal extinction curve (e.g., van de Hulst, 15) $A_V=4.3\times E_{(b-y)}$, so that in this case $E_{(B-V)}=1.3\times E_{(b-y)}$. In Fig. 3 we have plotted the values of $1.3\times E_{(b-y)}$ against the values of A_V determined from the Walraven colours. The agreement between the two studies shows the validity of the procedure used in this study. It should be noted that we can *not* infer the value of R from Fig. 3, since it was assumed in the calculation of A_V. However, Fig. 3 does show that the colours of the stars in our programme are consistent with a normal extinction curve.

In order to determine the distance modulus we need the apparent visual magnitude in the Johnson system, because the Straižys and Kuriliene grids give the absolute magnitude in the Johnson system. A transformation formula was calculated by Pel (1987, private communication), to derive m_V from V_W and $(V-B)$:

$$m_V=6.886-2.5\times V_W-0.082\times(V-B)\,. \tag{4}$$

The distance modulus is now derived from the relation: $5\times\log D-5=m_V-M_V-A_V$.

The two conversion formulae from the Walraven system to the Johnson system are based on empirical relations, so the errors can be estimated from the standard deviation of the points around the best fit. This results in: $\sigma(E_{(B-V)})=0\overset{m}{.}01$ and $\sigma(m_V)=0\overset{m}{.}015$. The error in $E_{(B-V)}$ results in a significant mean error in A_V of $0\overset{m}{.}03$. The error in the distance modulus is dominated by the error in M_V, so the mean error in the distance modulus is $0\overset{m}{.}3$.

The results are presented in Table 3. The first three columns give the identification of each star: column 1 is the HD number (HD), column 2 gives the running number in the SPECTER input catalogue for HIPPARCOS (HIPP), and column 3 gives the name. In columns 4 and 5 the galactic coordinates l and b are given. Columns 6–8 are the reddening-free parameters $[B-U]$, $[U-W]$, and $[B-L]$, respectively. In columns 9–11 $\log T_{\rm eff}$, $\log g$ and $\log L/L_\odot$ are presented. Column 12 is the apparent magnitude in the Johnson system as calculated from the Walraven V-intensity. Column 13 shows the absolute magnitude and column 14 the visual extinction. Columns 15 and 16 give the distance modulus and distance respectively. Column 17 gives an indication of the membership: a proper-motion member is denoted by a capital letter M (Blaauw, 1946; Bertiau, 1958), and a photometric member by a small m. Non-members have a blank here. Column 17 gives the spectral-type according to the MK-classification (Buscombe, 1974, and later issues).

4. The Hertzsprung-Russel diagram

4.1. Empirical and theoretical diagrams

In Fig. 4 we have plotted the reddening-free two-colour diagram $[B-U]$ vs. $[B-L]$ for the whole set of programme stars. Because of the physical meaning of these two parameters (see Sect. 3.1), it is basically the observational counterpart of the $\log T_{\rm eff}$ vs. $\log g$ diagram. The line is the zero-age main-sequence (ZAMS) calculated from theoretical stellar evolution models (see Sect. 4.2). Figure 5 shows the HR-diagram in its basic form of $\log L/L_\odot$ vs. $\log T_{\rm eff}$. The results from the calculations described in Sects. 3.2 and 3.3 are plotted. Again the line is the ZAMS.

In Fig. 4 stellar evolution moves a star approximately to the lower left in the diagram. The ZAMS should therefore be the upper right boundary of the datapoints. It is clear that this is the case for the bulk of the stars in our programme. The spread away from the ZAMS, especially at lower temperatures, may be due to several effects. First of all the occurrence of peculiar features or emission lines in the spectrum of a star can influence the observed colours, thus giving it an abnormal position in the two-colour diagram. Secondly, a number of stars in the sample may be either pre-main-sequence objects or they may already have evolved away from the main sequence. Most of these objects turn out to be non-members. An exception to this is the A5 II star *o* Sco, which was shown by Blaauw et al. (1955) to be a proper-motion member of the Upper-Scorpius subgroup. Its location in the HR-diagram is entirely consistent with its spectral type, therefore its evolutionary state is inconsistent with the age of Upper Scorpius. A third cause for a shift in the two-colour diagram is duplicity. This is of

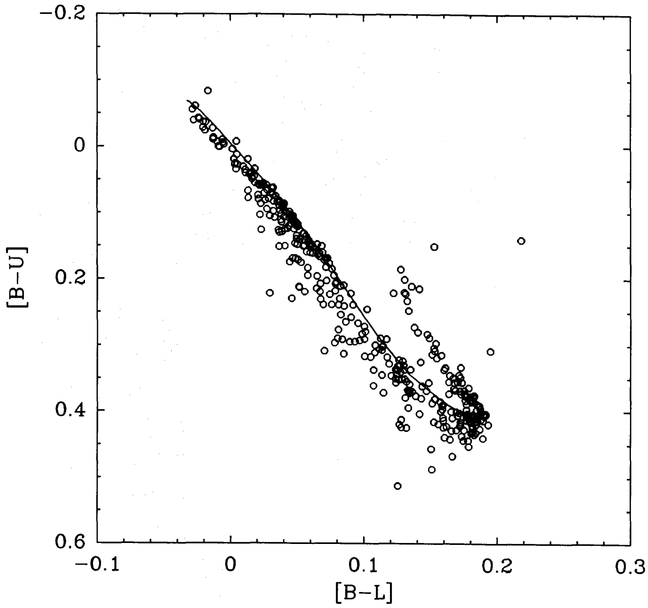

Fig. 4. Reddening-free two-clour diagram of all program stars in Scorpio-Centaurus. The line is the theoretical zero-age main-sequence, i.e. isochrone of age zero

Table 3a. Derived physical parameters for stars in Lower-Centaurus Crux

HD	Hipp	Name	l °	b °	[B – U]	[U – W]	[B – L]	log T_{eff}	log g	log $L/L_\odot$	m_V m	M_V m	A_V m	D.M. m	Dist. pc.	Mem.	MK Spectral Type
(1)	(2)	(3)	(4)	(5)	(6)	(7)	(8)	(9)	(10)	(11)	(12)	(13)	(14)	(15)	(16)	(17)	(18)
99264	7341		296.321	-10.515	0.0977	0.0223	0.0321	4.27	3.80	3.5	5.57	-2.5	0.78	7.3	294		B 2 IV-V
99556	6775	θ^2 Cru	292.869	0.087	0.1512	0.0407	0.0365	4.19	3.32	3.7	5.28	-3.5	0.30	8.5	504		B 3 III/IV
100929	6777		293.977	0.507	0.1264	0.0292	0.0359	4.23	3.58	3.6	5.83	-2.9	0.28	8.5	509		B 2.5 IV
102776	6967		296.180	-1.729	0.1480	0.0302	0.0501	4.20	3.86	3.1	4.32	-1.7	0.06	6.0	158	m	B 3 V n e
103079	7022		296.738	-3.054	0.1602	0.0263	0.0692	4.19	4.36	2.5	4.89	-0.2	0.08	5.0	100	M	B 4 V
103884	€855		296.762	-0.223	0.1319	0.0237	0.0544	4.23	4.20	2.8	5.57	-0.8	0.05	6.3	186	M	B 3 V
104841	6913		297.647	-0.779	0.1241	0.0242	0.0427	4.23	3.88	3.3	4.72	-1.9	0.29	6.4	190	m	B 2 V
104878	7188		298.619	-5.850	0.3239	0.0670	0.1292	4.05	4.40	1.7	5.34	1.0	0.18	4.1	68		
105382	5992		295.946	11.621	0.1048	0.0118	0.0294	4.25	3.58	3.8	4.49	-3.2	0.14	7.6	335	M	B 2 III n e
105383	6111		295.962	11.521	0.3357	0.0705	0.1242	4.04	4.20	1.8	6.37	0.7	0.05	5.6	133	m	B 9 V
105416	5853		295.626	13.565	0.4239	0.1138	0.1280	3.98	3.54	2.3	5.34	-0.9	0.05	6.1	172	m	A 0 V
105435	6113	δ Cen	296.000	11.568	-0.0076	0.0220	0.0045	4.45	4.64	5.1	2.58	-4.0	0.41	6.1	171	M	B 2 IV n e
105580	6724		297.659	2.671	0.1591	0.0331	0.0572	4.19	4.00	2.9	7.14	-1.2	0.33	8.0	405		B 6 V
105937	6238	ρ Cen	296.787	10.028	0.1468	0.0237	0.0603	4.21	4.22	2.7	3.96	-0.6	0.01	4.6	83	M	B 3 V
106490	6663	δ Cru	298.232	3.791	0.0305	0.0051	0.0096	4.36	3.88	4.0	2.78	-3.2	0.05	5.9	153	M	B 2 IV n
107696	6557		299.103	4.983	0.2407	0.0555	0.0854	4.11	4.08	2.3	5.38	-0.2	0.05	5.6	132	m	B 7 V
108257	6133		298.983	11.230	0.1402	0.0285	0.0521	4.22	4.04	2.9	4.81	-1.2	0.06	6.0	159	M	B 3 V n
109026	7343	γ Mus	301.462	-9.316	0.1498	0.0353	0.0554	4.20	4.04	2.9	3.84	-1.1	0.04	4.9	98	M	B 5 V
109668	7237	α Mus	301.659	-6.299	0.0590	0.0098	0.0234	4.33	4.06	3.6	2.68	-2.2	0.06	4.8	92	M	B 2 IV-V n
110335	6732		301.735	3.164	0.2115	0.0766	0.0514	4.12	3.28	3.4	4.96	-2.9	0.35	7.5	326		B 5 III e
110879	7194	β Mus	302.452	-5.241	0.0929	0.0162	0.0394	4.28	4.18	3.1	3.04	-1.3	0.06	4.3	73	m	B 2 V
110956	6512		302.232	6.376	0.1318	0.0240	0.0551	4.23	4.24	2.8	4.63	-0.7	0.05	5.2	114	M	B 3 V
111123	6733	β Cru	302.465	3.180	-0.0070	-0.0012	-0.0099	4.39	3.50	4.7	1.24	-4.8	0.06	6.0	162	M	B 0.5 III
111613	6737		302.917	2.542	0.2218	0.1670	0.0294	4.07	2.34	4.5	5.73	-5.8	1.56	10.0	1019		B 9.5 Iab
112078	6682	λ Cru	303.348	3.723	0.1503	0.0311	0.0546	4.20	4.00	2.9	4.61	-1.2	0.05	5.8	147	M	B 4 V n e
112091	6570	μ^2 Cru	303.368	5.701	0.1713	0.0407	0.0704	4.18	4.28	2.4	5.17	-0.0	0.13	5.1	105	M	B 5 V n e
112092	6569	μ^1 Cru	303.365	5.691	0.0840	0.0153	0.0351	4.29	4.14	3.3	4.01	-1.5	0.08	5.5	126	M	B 2 IV-V
113314	5940	ξ^1 Cen	304.955	13.297	0.4287	0.1015	0.1657	3.96	3.98	1.6	4.84	0.8	0.00	4.0	63		
113703	5865		305.473	14.335	0.1616	0.0280	0.0668	4.19	4.26	2.5	4.70	-0.3	0.03	5.0	101	M	B 5 V
113791	6056	ξ^2 Cen	305.489	12.889	0.0730	0.0111	0.0318	4.31	4.18	3.3	4.27	0.0	0.08	4.1	68	M	B 1.5 V
115823	6369		307.411	9.870	0.1946	0.0396	0.0776	4.16	4.26	2.3	5.46	-0.0	0.03	5.4	123	M	B 6 V
115846	7149		305.807	-4.833	0.1514	0.0253	0.0598	4.20	4.16	2.7	7.04	-0.7	0.39	7.4	303		B 3 V
116072	6823		306.707	1.671	0.1073	0.0280	0.0329	4.25	3.70	3.6	6.20	-2.7	0.62	8.3	456		B 2.5 V n
116087	6822		306.710	1.655	0.1495	0.0258	0.0609	4.21	4.22	2.7	4.52	-0.6	0.07	5.0	103	M	B 3 V
116226	5870		308.314	13.978	0.2125	0.0648	0.0516	4.12	3.28	3.4	6.36	-2.9	0.20	9.1	659		B 6 IV
118716	6373	ϵ Cen	310.195	8.721	0.0192	0.0042	0.0025	4.37	3.68	4.3	2.29	-3.9	0.07	6.1	168	M	B 1 III n
118978	6698		309.460	3.442	0.3129	0.0883	0.0849	4.05	3.52	2.7	5.38	-1.6	0.22	6.7	226	m	
120908	6378		312.249	8.368	0.1944	0.0531	0.0578	4.15	3.66	3.1	5.87	-1.9	0.48	7.3	288		B 5 III
123335	6706		312.699	2.118	0.1348	0.0325	0.0496	4.22	4.00	3.0	6.34	-1.4	0.69	7.1	263		B 5 IV
124182	7105		311.210	-4.628	0.1287	0.0329	0.0386	4.22	3.66	3.5	6.94	-2.6	0.51	9.0	642		B 5 III
124197	7106		311.361	-4.201	0.1612	0.0281	0.0620	4.19	4.12	2.7	6.72	-0.7	0.40	7.1	264		B 3 V n

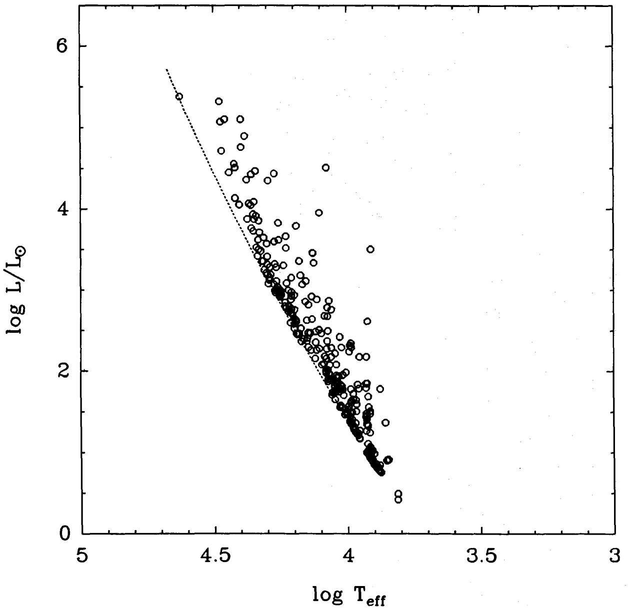

Fig. 5. Hertzsprung-Russell diagram of log $L/L_\odot$ vs. log T_{eff} for all programme stars. The line is the ZAMS

course dependent on the spectral type and brightness of the two components. If duplicity is known for an object, and the two components were observed together and their spectral types known, the colours can be corrected for this effect, giving the colours of the brighter one. If the magnitude difference is larger than 5^m, the correction is negligible. In our programme, for most stars for which duplicity is known we could either observe the components separately or the magnitude difference was large enough, so that no corrections were necessary. For stars of which duplicity is undetected, the colours may be influenced. A fourth effect, that of rotation, is important in the Strömgren system (Collins and Sonneborn, 1977; de Zeeuw and Brand, 1985), and was thought to cause an effect on the colours in the Walraven system (BW). However, a recent study by van de Grift (1987, MSc Thesis) shows that no correlation is apparent between the displacement away from the ZAMS and the rotational velocity of the star. This point needs further study.

4.2. *Isochrones*

In order to study the evolutionary stage of a group of stars, or the actual age, one compares the position of the stars in the HR-diagram with isochrones, i.e., lines connecting points of equal age.

Table 3b. Derived physical parameters for stars in Upper-Centaurus Lupus

HD	Hipp	Name	l	b	[B – U]	[U – W]	[B – L]	log T_{eff}	log g	log $L/L_\odot$	m_V	M_V	A_V	D.M.	Dist.	Mem.	MK Spectral Type
			°	°							m	m	m	m	pc.		
(1)	(2)	(3)	(4)	(5)	(6)	(7)	(8)	(9)	(10)	(11)	(12)	(13)	(14)	(15)	(16)	(17)	(18)
118335	4389		312.935	24.885	0.4078	0.0918	0.1768	3.97	4.30	1.3	7.65	1.5	0.01	6.0	163	m	A 1 III
119103	4834		312.647	18.769	0.3609	0.0938	0.1072	4.02	3.66	2.4	7.13	-0.8	0.04	7.9	392		B 8 III
119221	4835		312.772	18.704	0.3886	0.0987	0.1846	3.91	4.40	0.9	7.28	2.4	0.00	4.8	93	m	
119338	4447		314.036	23.492	0.1825	0.0371	0.0715	4.17	4.20	2.5	8.93	-0.3	0.10	9.1	674		B 5 V
119361	4731		313.200	19.761	0.2896	0.0793	0.0803	4.07	3.56	2.7	5.97	-1.6	0.08	7.4	313		
119430	4837		312.980	18.400	0.4247	0.1136	0.1318	3.98	3.58	2.2	7.10	-0.7	0.04	7.8	367		A 0 III
119674	4344		314.919	25.229	0.3786	0.1226	0.1821	3.92	4.44	1.0	9.04	2.2	0.54	6.2	177	m	A M
120307	4736	ν Cen	314.417	19.886	0.0399	0.0053	0.0153	4.35	4.02	3.7	3.41	-2.4	0.06	5.8	146	M	B 2 IV e
120324	4737	μ Cen	314.240	19.117	0.0704	0.0148	0.0254	4.31	3.94	3.6	3.46	-2.4	0.04	5.8	145	M	B 3 V p n e
120487	4637		314.801	20.496	0.3483	0.1068	0.1725	3.91	4.50	1.0	9.01	2.0	0.23	6.7	218	m	
120640	5248		313.530	14.728	0.0832	0.0138	0.0324	4.29	4.04	3.4	5.76	-1.8	0.17	7.4	304		B 2 V p
120709	4196	3 Cen	317.285	28.189	0.1119	0.0233	0.0465	4.26	4.18	3.0	4.49	-1.1	0.14	5.4	125	M	B 5 III p
120710	4195		317.287	28.188	0.3221	0.0628	0.1263	4.05	4.34	1.7	5.92	1.0	0.06	4.8	91	m	B 8 V n
120908	6378		312.249	8.368	0.1944	0.0531	0.0578	4.15	3.66	3.1	5.87	-1.9	0.48	7.3	288	M	B 5 III
120955	4164	4 Cen	317.930	29.139	0.1752	0.0433	0.0530	4.17	3.68	3.1	4.74	-1.9	0.05	6.6	217	M	B 4 IV
120959	4510		315.814	21.950	0.4437	0.1300	0.1746	3.92	3.78	1.8	8.74	0.2	0.13	8.4	477		A 3 V
120960	4744		315.206	19.753	0.2888	0.1030	0.1491	3.87	4.46	0.7	7.86	2.8	0.21	4.8	91	m	
121057	5421		313.509	12.883	0.4135	0.1100	0.1893	3.91	4.25	1.0	7.19	2.1	0.06	5.0	101	m	
121190	5668		312.770	9.489	0.2907	0.0576	0.1169	4.07	4.44	1.9	5.66	0.6	0.04	5.0	101	m	B 8 V
121226	5252		314.069	14.396	0.4323	0.1063	0.1805	3.92	3.96	1.4	7.44	1.0	-0.05	6.4	193	m	
121292	5347		313.947	13.627	0.2792	0.0592	0.1011	4.08	4.16	2.0	9.01	0.2	0.17	8.6	533		
121399	4511		316.303	21.781	0.3809	0.0872	0.1531	4.00	4.28	1.5	7.20	1.2	1.30	4.6	84	m	
121528	4641		316.054	20.343	0.3339	0.1282	0.1611	3.89	4.38	0.8	9.21	2.6	0.40	6.1	169	m	
121743	4750	ϕ Cen	315.979	19.072	0.0591	0.0096	0.0243	4.33	4.10	3.6	3.81	-2.2	0.03	5.9	157	M	B 2 IV
121790	5031	υ^1 Cen	315.289	16.449	0.0696	0.0117	0.0309	4.31	4.20	3.3	3.85	-1.5	0.03	5.4	120	M	B 2 IV-V
121983	4201		318.904	27.206	0.0669	0.0309	0.0132	4.29	3.36	4.3	8.09	-4.3	0.35	12.1	2629		B 3 III
122109	4353		318.339	25.012	0.4391	0.1133	0.1606	3.96	3.80	1.8	8.02	0.4	0.02	7.5	325		A 2 V
122159	5354		314.668	12.688	0.2827	0.0639	0.0987	4.08	4.08	2.1	8.58	-0.0	0.24	8.4	478		
122324	5789		312.846	5.488	-0.0432	0.0115	-0.0240	4.47	3.50	5.3	9.09	-5.7	2.01	12.8	3714		B 0.5 Ia
122449	5263		315.479	14.305	0.2190	0.0543	0.0672	4.13	3.72	2.9	8.12	-1.5	0.19	9.5	798		B 5 III
122479	5678		314.045	9.251	0.1152	0.0200	0.0485	4.25	4.22	2.9	7.36	-0.9	0.38	7.9	393		
122664	4394		318.608	23.367	0.3736	0.1120	0.1732	3.91	4.30	0.9	8.35	2.2	0.17	5.9	152	m	
122705	5521		314.796	11.105	0.4037	0.0985	0.1898	3.95	4.42	1.1	7.65	1.8	0.16	5.6	133	m	A 4 V
122756	4651		317.444	19.512	0.2330	0.0963	0.1326	3.81	4.50	0.4	8.68	3.7	-0.19	5.1	108	m	
122757	4652		317.401	19.341	0.4209	0.1131	0.1813	3.92	4.06	1.3	8.65	1.3	0.03	7.2	281		A 4 V
122925	5752		313.822	7.077	0.2231	0.0544	0.0746	4.13	3.92	2.6	8.09	-0.8	0.32	8.6	535		
122980	4654	χ Cen	317.733	19.538	0.0819	0.0103	0.0364	4.30	4.24	3.2	4.35	-1.3	0.03	5.6	134	M	B 2 V
123021	4655		317.758	19.536	0.3369	0.1096	0.1602	3.89	4.32	0.8	8.35	2.6	0.11	5.6	134	m	A 1 V n
123130	5728		314.198	7.678	0.2388	0.0631	0.0812	4.11	3.98	2.4	8.71	-0.5	0.46	8.8	587		
123291	4939		317.180	16.753	0.3792	0.0893	0.1312	4.01	3.96	1.9	8.24	0.2	0.19	7.8	372		
123344	4304		320.188	25.351	0.3996	0.0939	0.1576	3.99	4.18	1.5	7.36	1.0	0.12	6.1	172	m	A 0 III
123431	4754		317.779	18.033	0.4092	0.0904	0.1592	3.98	4.10	1.6	8.73	0.8	0.01	7.8	373		
123635	4941		317.445	16.366	0.2479	0.1009	0.1338	3.81	4.25	0.4	11.73	3.5	0.22	7.9	395		
123635	4942		317.444	16.369	0.2387	0.0698	0.0697	4.11	3.64	2.8	7.74	-1.6	0.30	9.0	642		
123664	5151		316.964	14.802	0.4675	0.1275	0.1665	3.92	3.52	2.1	7.64	-0.6	0.11	8.1	427		A 2 IV.
124228	4585		319.541	20.236	0.4277	0.1211	0.1751	3.92	3.88	1.5	7.87	0.8	0.16	6.8	234	m	
124254	5155		317.529	14.543	0.3678	0.1091	0.1688	3.90	4.24	1.0	7.45	2.1	0.11	5.1	107	m	
124367	5802		314.128	3.960	0.0867	0.0377	0.0403	4.29	4.32	3.0	5.00	-1.0	0.48	5.5	130	m	B 5.. V n e
124504	4170		322.918	27.833	0.3767	0.1092	0.1765	3.91	4.34	0.9	8.13	2.3	0.26	5.5	129	m	
124540	4586		319.792	19.813	0.4526	0.1276	0.1787	3.92	3.75	1.8	9.02	0.2	0.20	8.5	523		

We have calculated isochrones for the evolutionary models of Maeder (1981a, b, c). We limited ourselves to his cases of zero mass-loss, and we used only the core-hydrogen-burning phase and the overall-contraction phase. These two cover basically the whole main-sequence strip in the HR-diagram. We used a linear interpolation between the points of the given age on the different evolutionary tracks. The interpolation was done in log $M/M_\odot$ in the (log $L/L_\odot$, log $M/M_\odot$) plane, and the (log $T_{\rm eff}$, log $M/M_\odot$) plane. Surface gravity was calculated from the basic formulae:

$$g = G\frac{M}{R^2}, \tag{5}$$

and

$$L = 4\pi R^2 \sigma T_{\rm eff}^4 \,. \tag{6}$$

Reddening-free colours were calculated from log g and log $T_{\rm eff}$ using the Kurucz grid (see Sect. 3.2). The zero-age main-sequence that was plotted in Figs. 4 and 5 is just the isochrone of age zero.

4.3. *Ages of the subgroups*

The isochrones can now be used to determine the so-called nuclear age of an OB association, i.e. the age according to the evolutionary state of the stars since they arrived on the ZAMS. The age of the isochrone fitting the observations of the stars best is taken as the age of the association or subgroup. The accuracy of the *absolute* age determined in this way unfortunately still depends on the model from which the isochrones were calculated. A comparison of different evolutionary models showed (de Geus, 1984) that models using the same basic input parameters have differences in for instance the main-sequence lifetime of 0.5 to 1.0 million years. The *relative* age determination however is much more accurate, because the evolutionary models are all internally consistent. Figures 6–8 show both the reddening-free colour-colour diagrams and the log $L/L_\odot$ vs. log $T_{\rm eff}$ diagrams for the three subgroups of Scorpio-Centaurus, with the best fitting isochrone drawn in. Note that in the age-determination the

Table 3b (continued)

HD (1)	Hipp (2)	Name (3)	l ° (4)	b ° (5)	[B − U] (6)	[U − W] (7)	[B − L] (8)	log T_{eff} (9)	log g (10)	log $L/L_\odot$ (11)	m_V m (12)	M_V m (13)	A_V m (14)	D.M. m (15)	Dist. pc. (16)	Mem. (17)	MK Spectral Type (18)
125238	5157	ι Lup	318.478	14.142	0.1065	0.0218	0.0402	4.26	4.02	3.2	3.54	-1.7	0.04	5.2	109	m	B 2 IV
125253	5158		318.482	14.097	0.4261	0.0960	0.1869	3.91	4.10	1.2	7.10	1.6	-0.22	5.7	138	m	
125509	4311		323.019	24.692	0.3947	0.0950	0.1332	4.00	3.88	1.9	7.71	0.0	0.03	7.6	332		B 9.5 III
125541	4763		320.380	18.164	0.2968	0.1053	0.1539	3.89	4.50	0.8	8.89	2.7	0.22	5.9	153	m	
125718	4764		320.462	17.734	0.4047	0.1152	0.1819	3.97	4.36	1.2	9.26	1.7	0.53	7.0	252		
125721	5367		318.200	11.830	-0.0071	0.0032	-0.0099	4.39	3.50	4.7	6.09	-4.8	0.39	10.5	1304		B 1 III
125823	4519		321.568	20.023	0.0902	0.0154	0.0392	4.28	4.22	3.1	4.41	-1.2	0.03	5.6	135	M	B 7 IIIp var H
125937	5161		319.362	14.241	0.3651	0.1091	0.1677	3.90	4.24	1.0	8.11	2.1	0.18	5.7	140	m	
126062	5272		318.934	12.778	0.4116	0.0926	0.1878	3.91	4.40	0.9	7.46	2.4	-0.33	5.3	118	m	
126194	4402		322.781	21.792	0.3689	0.0881	0.1722	3.91	4.32	0.9	6.70	2.3	-0.17	4.5	80	m	A 2 V
126341	5051	τ^1 Lup	319.921	14.504	0.0550	0.0118	0.0183	4.33	3.86	3.8	4.56	-2.8	0.24	7.1	273		B 2 II
126476	4589		321.933	18.889	0.4074	0.1146	0.1851	3.96	4.36	1.2	8.08	1.8	0.37	5.9	151	m	
126561	5166		319.779	13.491	0.4005	0.0815	0.1692	3.98	4.30	1.3	7.22	1.5	-0.02	5.7	140	m	
126981	5055		320.556	14.146	0.3165	0.0759	0.1006	4.05	3.86	2.2	5.51	-0.4	0.01	5.9	157	m	B 8 V n
127716	4771		322.558	16.826	0.4871	0.1542	0.1509	3.92	3.20	2.6	6.60	-1.7	0.04	8.3	457		A 3 IV
127717	4770		322.519	16.774	0.3134	0.1096	0.1512	3.87	4.26	0.8	9.05	2.5	0.21	6.2	178	m	
127778	4772		322.604	16.797	0.2831	0.1210	0.1474	3.87	4.48	0.7	9.86	2.8	0.52	6.4	196	m	
127879	4951		322.114	15.423	0.3452	0.1069	0.1645	3.90	4.36	0.8	7.85	2.6	0.14	5.0	104	m	A 5 V
127972	4773	η Cen	322.777	16.669	0.0777	0.0238	0.0133	4.27	3.20	4.4	2.44	-4.7	0.01	7.1	273	M	B 1.5 V n
128066	4669		323.217	17.373	0.2727	0.1027	0.1378	3.84	4.04	0.9	8.90	2.4	0.01	6.4	192	m	
128224	4407		325.430	21.562	0.2073	0.0550	0.0674	4.14	3.84	2.8	7.70	-1.2	0.18	8.7	563		
128344	5372		320.718	11.137	0.2947	0.0725	0.0894	4.07	3.76	2.4	6.66	-0.9	0.23	7.3	293		B 9 V
128532	4321		326.398	22.675	0.4198	0.1120	0.1839	3.95	4.25	1.2	6.78	1.6	0.32	4.8	93	m	
128788	4670		324.138	17.455	0.3766	0.1026	0.1821	3.92	4.46	1.0	8.31	2.2	0.14	5.9	152	m	
128819	4671		324.203	17.491	0.3056	0.0642	0.1116	4.06	4.18	1.9	6.65	0.4	0.04	6.2	173	m	
128855	4672		324.347	17.684	0.4565	0.1347	0.1506	3.95	3.52	2.1	7.36	-0.6	0.15	7.8	369		A 1 V
129056	5287	α Lup	321.613	11.437	0.0343	0.0089	0.0042	4.34	3.46	4.4	2.30	-4.3	0.08	6.6	209	M	B 1.5 III
129116	4468		325.904	20.100	0.1088	0.0193	0.0463	4.26	4.22	2.9	4.00	-1.0	0.04	4.9	99	M	B 3 V
129791	5064		323.368	13.413	0.3910	0.0896	0.1585	4.00	4.26	1.5	6.92	1.2	0.18	5.4	122	m	B 9.5 V
130163	4600		325.968	17.685	0.4240	0.1047	0.1598	3.97	3.96	1.7	6.92	0.6	0.06	6.2	175	m	B 9.5 V
130388	4367		328.344	21.454	0.4064	0.1118	0.1811	3.96	4.34	1.2	7.64	1.7	0.47	5.4	122	m	B 9.5 V
130807	4960	o Lup	324.901	14.110	0.1445	0.0356	0.0581	4.21	4.18	2.7	4.33	-0.7	0.04	5.0	102	M	B 5 IV
131120	4476		327.930	19.106	0.1026	0.0211	0.0438	4.27	4.22	3.0	5.02	-1.1	0.09	6.0	163	m	B 7 III p
131399	4280		330.118	22.156	0.4054	0.0924	0.1870	3.95	4.38	1.2	7.06	1.8	0.14	5.1	105	m	A 3 III
131460	4369		329.142	20.361	0.3493	0.1080	0.1670	3.90	4.38	0.8	8.99	2.5	0.36	6.0	164	m	
131461	4370		329.013	20.112	0.4054	0.0852	0.1786	3.97	4.34	1.2	7.24	1.6	0.12	5.4	122	m	A 1 IV
131503	4973		325.160	13.121	0.3972	0.1207	0.1768	3.98	4.40	1.3	8.00	1.5	0.68	5.7	139	m	
131518	4974		325.155	13.057	0.3563	0.1127	0.1679	3.90	4.34	0.9	9.14	2.4	0.35	6.3	182	m	
131752	4538		327.791	17.340	0.3898	0.0910	0.1593	4.00	4.28	1.4	6.36	1.3	0.24	4.7	90	m	
131777	4780		326.322	14.641	0.4164	0.0994	0.1799	3.92	4.06	1.3	8.15	1.3	-0.13	6.9	240	m	
131901	4231		331.394	22.989	0.4280	0.1037	0.1693	3.96	4.02	1.5	7.20	0.9	0.22	6.0	161	m	
132058	4874	β Lup	326.255	13.910	0.0398	0.0079	0.0112	4.34	3.76	4.0	2.68	-3.3	0.05	5.9	156	M	B 2 III
132080	4781		326.917	15.028	0.3558	0.1146	0.1737	3.91	4.48	0.9	9.71	2.4	0.40	6.8	238	m	
132094	4422		329.173	18.957	0.3700	0.0804	0.1363	4.02	4.12	1.7	7.27	0.7	0.04	6.5	199	m	
132200	4782	κ Cen	326.874	14.754	0.0791	0.0140	0.0288	4.30	3.94	3.5	3.13	-2.2	0.04	5.3	118	M	B 2 IV
132761	4185		333.001	23.608	0.3734	0.1063	0.1755	3.91	4.34	0.9	7.75	2.3	0.23	5.1	108	m	
132851	4051	60 Hya	335.098	26.529	0.4303	0.1239	0.1817	3.92	3.98	1.4	5.84	1.1	0.22	4.4	78		A 5 V
132955	4237		332.606	22.541	0.1415	0.0241	0.0587	4.22	4.24	2.7	5.44	-0.6	0.14	5.9	152	M	B 3 V
133574	4331		331.680	19.829	0.3083	0.1040	0.1531	3.88	4.38	0.7	8.72	2.7	0.23	5.7	138	m	
133716	4485		330.423	17.580	0.4371	0.1116	0.1733	3.92	3.78	1.6	7.18	0.5	-0.11	6.7	224	m	

chemically peculiar stars were given zero weight when fitting the isochrone. It is clear that the derived age for Lower-Centaurus Crux is least well determined, due to the large spread in the colours of the stars at the high-mass end of the diagram. In Table 4 we list the derived nuclear ages, and compare them with nuclear ages found by de Zeeuw and Brand (1985), and for Upper-Scorpius with the kinematic age determined by Blaauw (1964, 1978), based on proper motion studies of the stars. Our nuclear ages are close to the ages determined by de Zeeuw and Brand (1985), the difference can be explained by the differences in the stellar evolution models used to calculate the isochrones. For Upper-Scorpius the photometric age corresponds well with the kinematic age. Furthermore, we note that within the observational errors there is no evidence for a spread in age within a subgroup.

Table 4. Nuclear and kinematic ages

	τ_{nuc} (*VBLUW*) [10^6 yr]	τ_{nuc} ($uvby\beta$) [10^6 yr]	τ_{kin} [10^6 yr]
Upper Scorpius	5– 6	6– 8	5
Upper-Centaurus Lupus	14–15	12–13	
Lower-Centaurus Crux	11–12	10–11	

Note: Column 1 lists the nuclear age derived from the Walraven data. Column 2 gives the nuclear age as given by de Zeeuw and Brand (1985). For comparison, column 3 shows the kinematic age (only available for Upper-Scorpius) given by Blaauw (1964, 1978). Note that the nuclear age derived from the Walraven photometric data is consistent with the kinematic age

Table 3b (continued)

HD	Hipp	Name	l °	b °	[B − U]	[U − W]	[B − L]	log T_{eff}	log g	log $L/L_{\odot}$	m_V m	M_V m	A_V m	D.M. m	Dist. pc.	Mem.	MK Spectral Type
(1)	(2)	(3)	(4)	(5)	(6)	(7)	(8)	(9)	(10)	(11)	(12)	(13)	(14)	(15)	(16)	(17)	(18)
133750	4238		333.270	21.843	0.4219	0.0919	0.1721	3.96	4.10	1.5	7.18	1.1	0.08	5.9	156	m	B 8 V
133937	4886		328.040	13.216	0.2178	0.0470	0.0787	4.13	4.08	2.4	5.82	-0.4	0.04	6.2	174	M	B 7 V nn
133955	5071	λ Lup	326.802	11.129	0.1199	0.0196	0.0494	4.24	4.18	2.9	4.06	-1.0	0.04	5.0	104	M	B 3 V
134055	4541		330.440	16.879	0.3449	0.1021	0.1714	3.91	4.50	1.0	7.25	2.0	0.26	4.9	95	m	
134518	4377		332.141	18.560	0.3682	0.1147	0.1754	3.91	4.40	0.9	9.28	2.4	0.48	6.4	190	m	
134685	4334		333.034	19.541	0.4096	0.0969	0.1663	3.98	4.18	1.4	7.68	1.1	0.40	6.1	167	m	A 0 V
134687	5075		327.831	11.430	0.1177	0.0205	0.0495	4.25	4.22	2.9	4.82	-0.9	0.03	5.7	141	m	B 3 IV
134930	4978		328.392	11.920	0.3824	0.1000	0.1818	3.92	4.40	1.0	7.37	2.2	0.14	4.9	99	m	
134950	4380		332.800	18.650	0.4148	0.1144	0.1853	3.95	4.25	1.2	8.33	1.6	0.62	6.1	165	m	
134990	4547		331.349	16.380	0.4161	0.1117	0.1725	3.91	3.90	1.4	7.07	1.0	-0.05	6.0	163	m	
135454	4793		329.588	12.866	0.3801	0.0868	0.1431	4.01	4.14	1.7	6.76	0.8	0.01	5.8	150	m	B 9 V
135814	4699		330.771	13.948	0.3150	0.1138	0.1581	3.89	4.48	0.8	8.72	2.7	0.24	5.7	143	m	
135877	4701		330.551	13.485	0.4223	0.1349	0.1618	3.97	4.02	1.6	8.74	0.7	0.62	7.3	293		
136013	4287		334.866	19.510	0.4130	0.0878	0.1770	3.96	4.24	1.3	7.77	1.4	0.15	6.1	169	m	A 1 V
136164	4337		334.483	18.675	0.3832	0.1026	0.1761	3.91	4.28	1.0	7.79	2.1	0.11	5.5	127	m	
136298	4704	δ Lup	331.324	13.816	0.0351	0.0068	0.0110	4.36	3.86	4.0	3.22	-3.1	0.05	6.3	185	M	B 1.5 IV
136334	4705		331.301	13.709	0.4313	0.1033	0.1811	3.92	3.96	1.4	6.20	1.0	-0.10	5.2	111	m	
136482	4494		333.212	16.219	0.3279	0.0722	0.1189	4.05	4.16	1.9	6.65	0.4	0.02	6.1	169	m	
136483	4706		331.333	13.474	0.3251	0.1561	0.1426	3.85	3.72	1.3	8.93	1.2	0.54	7.1	264		
136504	5078	ϵ Lup	329.230	10.323	0.0895	0.0168	0.0366	4.28	4.12	3.2	3.38	-1.5	0.04	4.9	95	m	B 3 IV
136664	4438	ϕ^2 Lup	333.839	16.748	0.1356	0.0246	0.0566	4.22	4.24	2.7	4.54	-0.6	0.04	5.1	108	M	B 4 V
136961	4385		334.669	17.340	0.4320	0.1117	0.1804	3.92	3.96	1.4	6.75	1.0	-0.10	5.8	144	m	
137169	4709		332.132	13.404	0.4437	0.1275	0.1782	3.92	3.80	1.7	8.98	0.3	0.23	8.3	475		
137193	4613		332.535	13.931	0.3015	0.0972	0.1142	4.07	4.28	1.8	7.38	0.6	0.27	6.4	192	m	A 0 p Si
137432	4441		334.600	16.343	0.1590	0.0323	0.0645	4.19	4.22	2.6	5.46	-0.5	0.02	5.9	156	M	B 4 V p shell
137785	4558		333.806	14.594	0.2801	0.1078	0.1404	3.85	4.10	0.9	6.45	2.4	0.07	3.8	59		
137957	5081		330.008	8.905	0.4419	0.1132	0.1647	3.95	3.82	1.7	7.46	0.4	0.11	6.8	236	m	
138285	4502		334.672	14.680	0.4036	0.0850	0.1776	3.97	4.36	1.3	7.50	1.6	0.00	5.8	148	m	A 2 V
138564	4563		334.183	13.440	0.3807	0.0726	0.1535	4.00	4.28	1.5	6.37	1.2	-0.02	5.1	106	m	
138690	4714	γ Lup	333.196	11.892	0.0592	0.0109	0.0217	4.32	3.96	3.7	2.77	-2.4	0.05	5.2	110	M	B 2 IV
138769	5085		331.019	8.760	0.1167	0.0203	0.0488	4.25	4.20	2.9	4.55	-1.0	0.00	5.6	132	M	B 3 IV p shell
138940	4716		333.507	11.797	0.3677	0.0802	0.1330	4.02	4.08	1.8	7.63	0.6	0.02	7.0	251	m	
139048	4565		334.993	13.515	0.3190	0.1131	0.1546	3.88	4.32	0.8	9.12	2.6	0.32	6.1	166	m	
139233	4566		334.965	13.102	0.3404	0.0694	0.1276	4.04	4.24	1.7	6.59	0.8	-0.02	5.7	142	m	B 9 V
139524	5002		332.100	8.849	0.3371	0.0795	0.1073	4.04	3.86	2.2	8.05	-0.3	0.27	8.1	424		
140008	3862	ψ^2 Lup	338.484	16.084	0.1764	0.0332	0.0742	4.18	4.34	2.4	4.74	-0.1	0.00	4.8	92	M	B 5 IV
140602	5005		333.051	8.327	0.3956	0.1040	0.1872	3.91	4.40	0.9	8.26	2.4	-0.01	5.8	148	m	
142201	4626		336.815	10.366	0.3764	0.1059	0.1389	4.01	4.10	1.7	10.51	0.7	0.81	8.9	625		
143118	3970	η Lup	338.776	11.009	0.0460	0.0100	0.0162	4.34	3.92	3.8	3.43	-2.8	0.03	6.2	175	M	B 2.5 IV
143699	3971		339.122	10.427	0.1534	0.0352	0.0626	4.20	4.22	2.7	4.90	-0.5	0.04	5.4	122	M	B 6 IV
144294	3928	θ Lup	340.836	11.323	0.1082	0.0200	0.0440	4.26	4.14	3.1	4.22	-1.2	0.03	5.4	124	M	B 2.5 V n

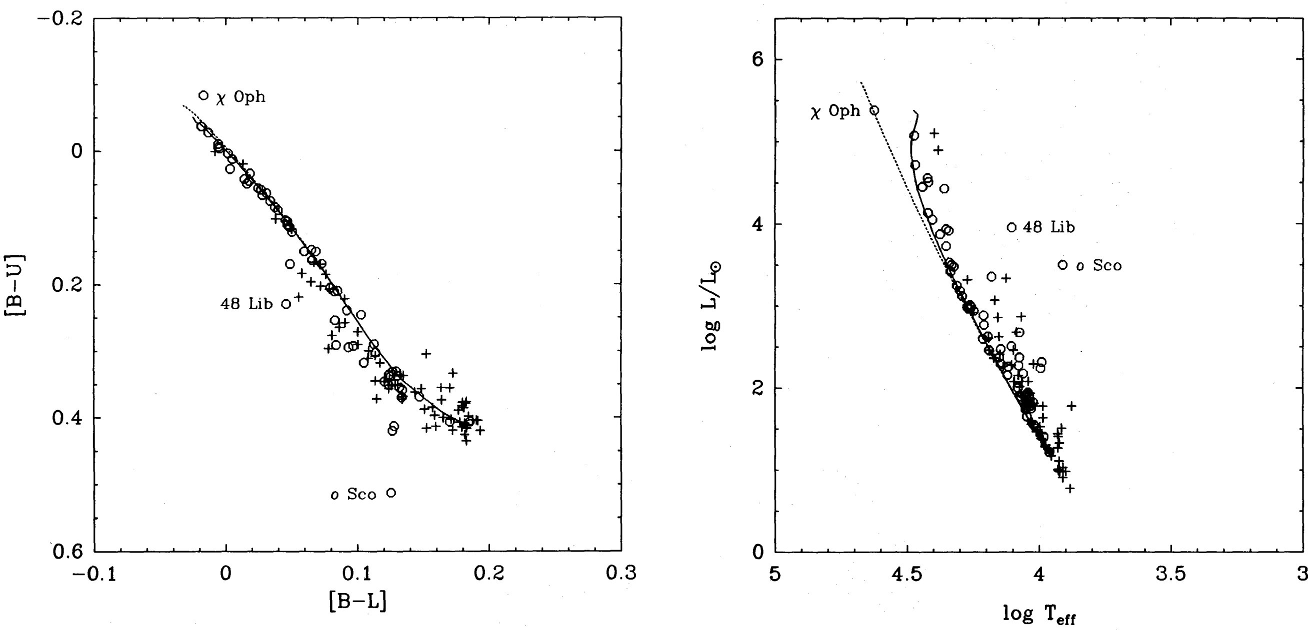

Fig. 6a. Reddening-free two-colour diagram of the stars in the Upper-Scorpius subgroup. Circles denote the established members of the association, plusses denote the remaining programme stars. The dashed line shows the ZAMS, whereas the full line gives the isochrone of age 5.5 million years

Fig. 6b. HR-diagram of the stars in the Upper-Scorpius subgroup. Circles denote the established members of the association, plusses denote the remaining programme stars. Note that the three member stars with strongly deviating position in the diagram are stars with a peculiar, emission-line spectrum (χ Oph and 48 Lib), and the bright giant o Sco (A 5II)

Table 3c. Derived physical parameters for stars in Upper Scorpius

HD (1)	Hipp (2)	Name (3)	l ° (4)	b ° (5)	[B − U] (6)	[U − W] (7)	[B − L] (8)	log T_{eff} (9)	log g (10)	log $L/L_\odot$ (11)	m_V m (12)	M_V m (13)	A_V m (14)	D.M. m (15)	Dist. pc. (16)	Mem. (17)	MK Spectral Type (18)
138138	3830		337.116	18.236	0.3757	0.1021	0.1829	3.92	4.50	1.0	6.88	2.2	0.07	4.5	82	m	
139094	3394		343.037	23.198	0.2390	0.0537	0.0920	4.12	4.26	2.1	7.40	0.2	0.59	6.5	203	M	B 7 V
139365	3622		341.067	20.448	0.1139	0.0202	0.0485	4.25	4.22	2.9	3.66	-1.0	0.03	4.6	85	M	B 2.5 V
139486	2945		348.324	28.014	0.3685	0.0729	0.1470	4.01	4.30	1.5	7.63	1.2	0.22	6.1	168	M	B 9.5 V
140475	3865		338.626	15.467	0.4035	0.0942	0.1905	3.95	4.40	1.1	7.72	1.8	0.10	5.7	142	m	A 5 III
140817	3890		338.678	14.897	0.3563	0.0753	0.1487	4.02	4.44	1.5	6.84	1.3	0.16	5.3	118	m	
140958	3947		336.999	12.677	0.3552	0.1045	0.1704	3.91	4.40	0.9	8.08	2.4	0.11	5.4	125	m	
141180	3492		344.381	20.686	0.2997	0.0630	0.1085	4.07	4.16	2.0	8.28	0.3	0.20	7.7	358		B 8 V
141404	3000		349.573	25.541	0.4198	0.1162	0.1265	3.98	3.56	2.3	7.72	-0.8	0.51	8.0	399	M	B 9.5 IV
141556	3835	χ Lup	340.572	15.818	0.3721	0.0907	0.1341	4.01	4.08	1.8	3.97	0.6	-0.01	3.3	46		B 9 IV p Sr Eu
141637	3321	1 Sco	346.099	21.706	0.0580	0.0086	0.0268	4.33	4.22	3.4	4.64	0.0	0.49	4.1	67	M	B 1.5 V n
141774	3001		350.060	25.381	0.3504	0.0776	0.1238	4.03	4.08	1.9	7.71	0.4	0.45	6.8	232	M	B 9 V
141905	3986		336.722	10.777	0.4349	0.1207	0.1828	3.92	4.00	1.4	8.33	1.1	0.43	6.7	222	m	
141939	3401		345.437	20.456	0.4041	0.1051	0.1916	3.95	4.40	1.1	8.25	1.8	0.44	5.9	154	m	
142097	3038		349.344	24.084	0.3783	0.1025	0.1824	3.92	4.46	1.0	8.43	2.2	0.75	5.4	122	m	
142114	3247	2 Sco	346.879	21.614	0.1037	0.0162	0.0453	4.27	4.26	2.9	4.60	-1.0	0.36	5.2	112	M	B 2 V n
142165	3248		347.516	22.148	0.2049	0.0396	0.0795	4.15	4.22	2.3	5.38	-0.0	0.36	5.0	102	m	B 6 IV n
142184	3169		347.934	22.545	0.1054	0.0252	0.0469	4.26	4.28	2.9	5.40	-0.9	0.49	5.8	147	M	B 2.5 V n
142250	3402		345.570	20.005	0.2094	0.0416	0.0850	4.14	4.32	2.4	6.15	-0.1	0.16	6.1	167	M	B 6 V p
142315	3095		348.982	23.299	0.3022	0.0609	0.1137	4.07	4.26	1.9	6.86	0.6	0.37	5.8	149	M	B 8 V
142378	2911	47 Lib	351.648	25.658	0.1479	0.0228	0.0652	4.21	4.38	2.5	5.95	-0.3	0.44	5.8	146	M	B 5 V
142431	4000		336.636	9.784	0.4156	0.1083	0.1829	3.92	4.14	1.2	7.07	1.5	0.01	5.4	124	m	
142669	3572	ρ Sco	344.631	18.271	0.0661	0.0125	0.0276	4.32	4.12	3.4	3.88	-1.8	0.07	5.7	138	M	B 2 IV-V
142805	3043		350.414	23.806	0.4125	0.1090	0.1279	3.99	3.64	2.2	7.15	-0.5	0.61	7.1	267	M	A 0 III
142883	3004		350.886	24.086	0.1503	0.0239	0.0685	4.21	4.46	2.8	5.84	-1.0	0.55	6.3	182	M	B 3 V
142884	3173		348.965	22.254	0.1664	0.0368	0.0670	4.19	4.22	2.6	6.78	-0.4	0.51	6.7	219	m	B 9 V p Si
142983	2809	48 Lib	356.388	28.632	0.2294	0.0685	0.0460	4.10	2.96	3.9	4.91	-4.3	0.14	9.1	673	M	B 5 III pe sh
142990	3252		348.121	21.197	0.1105	0.0247	0.0469	4.26	4.22	3.0	5.43	-1.0	0.29	6.2	174	M	B 4 IV p
143018	3330	π Sco	347.217	20.231	0.0121	0.0010	0.0047	4.40	4.04	4.0	2.89	-2.9	0.23	5.6	133	M	B 1 V
143275	3098	δ Sco	350.099	22.491	-0.0103	-0.0002	-0.0060	4.44	3.92	4.4	2.32	-3.8	0.47	5.6	135	M	B 0.3 IV
143567	3045		350.873	22.681	0.3371	0.0689	0.1303	4.04	4.32	1.6	7.21	1.1	0.48	5.5	130	M	B 9 V
143600	3099		350.381	22.135	0.3587	0.0802	0.1343	4.02	4.18	1.7	7.34	0.8	0.44	6.0	164	M	B 9 V n
143692	3100		350.096	21.700	0.4141	0.1136	0.1793	3.92	4.06	1.3	7.98	1.4	0.27	6.2	181	m	
144217	2956	β^1 Sco	353.195	23.600	-0.0036	-0.0026	-0.0049	4.42	3.78	4.5	2.72	-4.1	0.55	6.3	186	M	B 0.5 V
144218	2957	β^2 Sco	353.198	23.601	0.0750	0.0112	0.0338	4.31	4.24	3.2	4.94	0.0	0.58	4.3	74	M	B 2 IV-V
144334	3180		350.349	20.855	0.1505	0.0347	0.0597	4.20	4.16	2.7	5.92	-0.7	0.26	6.4	192	M	B 5 V
144470	3010	ω^1 Sco	352.752	22.773	0.0039	0.0002	0.0016	4.42	4.06	4.1	3.95	-3.0	0.70	6.3	183	M	B 1 V
144661	3254		349.996	19.969	0.1635	0.0377	0.0656	4.19	4.22	2.6	6.33	-0.4	0.31	6.5	199	M	B 7 IIIP He-wk
144844	3184		350.736	20.368	0.2455	0.0466	0.1027	4.11	4.48	2.2	5.88	0.3	0.37	5.2	110	M	B 9 IV0 p
144941	3418		348.142	17.753	0.0194	0.0478	0.0129	4.39	4.36	5.1	10.14	-4.0	0.83	13.3	4594		
145102	3419		348.548-	17.871	0.3176	0.0756	0.1051	4.06	3.96	2.1	6.61	-0.1	0.46	6.3	184	M	B 9 V p Si
145353	3420		348.578	17.496	0.3458	0.0751	0.1206	4.04	4.08	1.9	6.95	0.3	0.60	6.0	158	M	B 9 IV
145468	3102		352.151	20.629	0.3889	0.1070	0.1769	3.99	4.50	1.3	8.23	1.5	0.99	5.7	138	m	
145482	3508		348.118	16.836	0.0842	0.0155	0.0374	4.29	4.24	3.1	4.58	-1.3	0.14	5.7	140	M	B 2 V
145483	3582		347.747	16.498	0.3304	0.0709	0.1298	4.05	4.36	1.7	5.68	1.0	0.19	4.4	78	M	B 9 V n
145501	2959	ν Sco^C	354.616	22.711	0.1849	0.0430	0.0760	4.17	4.30	2.3	6.28	0.0	0.79	5.4	120	m	B 9 III (B 8 V)
145502	2960	ν Sco^A	354.611	22.701	0.0630	0.0060	0.0308	4.33	4.32	3.5	4.01	-1.6	0.79	4.8	91	M	B 2 IV p
145519	2916		354.948	22.950	0.3377	0.0712	0.1252	4.04	4.22	1.8	8.00	0.7	0.95	6.2	181	M	B 9 V n
145554	2961		354.579	22.557	0.3308	0.0634	0.1269	4.05	4.30	1.7	7.65	0.9	0.65	6.0	161	M	B 9 V n
145556	3509		347.891	16.492	0.2191	0.0705	0.0556	4.12	3.36	3.3	8.90	-2.6	0.60	10.9	1542		B 6 V

5. Properties of the Scorpio-Centaurus OB association

5.1. Distance to the subgroups; photometric membership determination

In order to determine the distance and the distance spread of the three subgroups, we will use only the stars for which membership is established by the proper motion studies of Blaauw (1946) and Bertiau (1958). However we will not include stars with peculiar spectra or emission lines, because these will have spectral energy distributions deviating from the normal one, which influences the colours.

Figure 9 shows the distance modulus as a function of galactic longitude for the member stars with normal spectra. Projected onto the Galactic plane, the three subgroups show a very smooth distribution, which strongly supports the idea that the groups in the Scorpio-Centaurus OB association have a common origin. The average distances to the three subgroups are listed in Table 5.

Table 5. Photometric and astrometric distances (D.M. is the distance modulus)

	D.M. (Phot) [mag]	D.M. (Astr) [mag]
Upper Scorpius	6.0±0.8	6.0±0.3
Upper-Centaurus Lupus	5.8±0.7	5.7±0.3
Lower-Centaurus Crux	5.4±0.6	5.6±0.4

Note: Column 1 lists the distance moduli as derived from the Walraven photometric data, and column 2 shows the distance moduli based on astrometric measurements (Jones, 1970). Note the excellent correspondence between the photometric and astrometric distances to the subgroups

Table 3c (continued)

HD	Hipp	Name	l °	b °	[B – U]	[U – W]	[B – L]	log $T_{\rm eff}$	log g	log $L/L_\odot$	m_V m	M_V m	A_V m	D.M. m	Dist. pc.	Mem.	MK Spectral Type
(1)	(2)	(3)	(4)	(5)	(6)	(7)	(8)	(9)	(10)	(11)	(12)	(13)	(14)	(15)	(16)	(17)	(18)
145631	2962		354.703	22.543	0.3546	0.0753	0.1320	4.03	4.18	1.7	7.60	0.7	0.61	6.2	176	M	B 9.5 V n
145792	3259		351.012	19.029	0.1688	0.0280	0.0728	4.18	4.38	2.4	6.41	-0.1	0.54	5.9	155	M	B 5 V
145793	3512		348.143	16.345	0.3851	0.0996	0.1806	3.92	4.36	0.9	7.95	2.2	0.31	5.3	118	m	A 3 V
146001	3341		350.389	18.118	0.2104	0.0411	0.0825	4.14	4.26	2.2	6.07	0.1	0.49	5.4	123	M	B 7 IV
146029	3104		352.785	20.231	0.3695	0.0780	0.1337	4.02	4.08	1.8	7.39	0.6	0.39	6.3	189	M	B 9 V
146284	3186		351.561	18.678	0.2944	0.0724	0.0932	4.07	3.86	2.3	6.70	-0.5	0.77	6.5	201	M	B 8 V
146285	3260		351.012	18.201	0.2896	0.0580	0.1125	4.08	4.34	2.0	7.93	0.5	0.95	6.4	193	M	B 9 V
146332	3646		347.490	14.850	0.1691	0.0553	0.0488	4.18	3.60	3.3	7.63	-2.4	1.08	8.9	626	M	B 5 III
146416	3016		353.983	20.598	0.3361	0.0700	0.1239	4.04	4.20	1.8	6.60	0.7	0.24	5.6	135	M	B 9 V
146606	3513		348.984	15.807	0.3849	0.0818	0.1572	4.00	4.30	1.4	7.07	1.3	0.02	5.6	136	m	A 0 V
146706	3107		352.676	19.019	0.3434	0.0759	0.1245	4.04	4.16	1.8	7.53	0.6	0.56	6.3	187	m	B 9 V
146899	3425		350.082	16.384	0.3732	0.1151	0.1639	4.00	4.48	1.4	10.26	1.4	2.02	6.7	228	m	A 7 V
146998	3343		350.948	16.990	0.3332	0.0777	0.1727	3.91	4.50	1.0	9.57	2.1	1.43	5.9	156	m	A 2 p Sr
147009	2964		355.502	20.894	0.4061	0.0868	0.1703	3.98	4.26	1.4	8.07	1.4	0.87	5.8	144	M	B 9.5 V
147010	2965		355.497	20.882	0.2071	0.0836	0.0788	4.14	4.18	2.4	7.39	-0.1	0.85	6.7	218	m	A p
147012	3345		351.162	17.133	0.3509	0.0772	0.1308	4.03	4.20	1.7	9.80	0.7	1.71	7.3	289		B 9 V
147013	3344		351.125	17.119	0.4022	0.0890	0.1714	3.98	4.30	1.3	9.10	1.5	1.26	6.3	182	m	A 0 V
147084	3188	o Sco	352.329	18.050	0.5125	0.2411	0.1255	3.91	2.42	3.5	4.57	-4.0	2.48	6.1	169	M	A 5 II
147105	3346		351.409	17.194	0.3873	0.1142	0.1511	3.87	3.52	1.7	8.83	0.2	0.84	7.7	357		A 0 p Sr Cr e
147165	3347	σ Sco	351.315	16.999	-0.0058	-0.0049	-0.0058	4.42	3.76	4.5	2.90	-4.3	1.20	6.0	159	M	B 1 III
147196	3189		352.800	18.244	0.2926	0.0684	0.0968	4.07	3.96	2.2	7.05	-0.3	0.79	6.5	207	M	B 8 IV
147283	3264		352.288	17.608	0.4193	0.1037	0.1932	3.92	4.25	1.1	10.32	1.9	2.23	6.1	166	m	A 3 V
147343	3265		352.451	17.634	0.3999	0.0960	0.1654	3.98	4.26	1.4	9.37	1.3	2.06	5.9	154	m	A 1 V n
147384	3266		352.480	17.573	0.3966	0.0867	0.1588	3.99	4.22	1.5	8.61	1.1	1.24	6.1	172	m	B 9.5 V
147432	3110		353.511	18.373	0.3771	0.0908	0.1799	3.92	4.42	0.9	7.55	2.2	0.36	4.9	96	m	A 2 V
147592	3349		351.202	16.111	0.4056	0.0867	0.1856	3.96	4.38	1.2	8.93	1.8	0.76	6.3	188	M	A 1 V
147648	3351		351.905	16.641	0.2575	0.0610	0.0906	4.10	4.08	2.2	9.47	-0.1	2.65	7.0	251	m	B 8 V
147649	3350		351.358	16.153	0.3823	0.0931	0.1795	3.92	4.36	0.9	9.64	2.3	0.94	6.4	190	m	A 7 V
147701	3267		352.257	16.849	0.1697	0.0343	0.0716	4.18	4.34	2.4	8.38	-0.1	2.17	6.3	182	m	B 5 V
147702	3352		351.738	16.382	0.3980	0.0955	0.1845	3.97	4.48	1.2	9.16	1.6	1.31	6.1	172	m	A 3 V
147703	3428		350.637	15.400	0.3682	0.0766	0.1347	4.02	4.12	1.7	7.48	0.7	0.66	6.1	167	m	B 9 V n
147809	3353		352.100	16.523	0.4072	0.0865	0.1779	3.97	4.32	1.3	8.62	1.6	1.17	5.8	147	m	A 1 V
147888	3191		353.649	17.709	0.1211	0.0106	0.0505	4.24	4.20	2.9	6.76	-0.9	1.50	6.2	177	M	B 5 V
147889	3268		352.859	17.044	0.0005	-0.0121	-0.0081	4.38	3.34	4.8	7.94	-5.2	3.34	9.8	931		B 4 V
147890	3653		349.098	13.696	0.2910	0.0907	0.0838	4.07	3.64	2.6	7.67	-1.3	0.98	8.0	401	M	B 8 p Si
147932	3194		353.721	17.715	0.1169	0.0164	0.0503	4.25	4.26	2.9	7.29	-0.8	1.48	6.6	218	m	B 5 V
147933	3192	ρ Oph^A	353.688	17.687	0.0269	-0.0031	0.0031	4.35	3.56	4.4	4.59	-2.1	1.45	5.3	114	M	B 2 IV-V
147934	3193	ρ Oph^B	353.689	17.688	0.0339	0.0014	0.0182	4.37	4.30	3.8	4.62	-2.3	1.40	5.5	129	M	B 2 IV-V
147955	3430		351.294	15.569	0.3367	0.0671	0.1350	4.04	4.40	1.7	8.09	1.0	0.94	6.1	169	m	B 9.5 V
148117	3432		351.327	15.269	0.3617	0.1101	0.1438	4.02	4.30	1.5	10.65	1.2	0.91	8.5	503		A 7 p Cr Eu
148118	3431		351.025	15.004	0.4254	0.1093	0.1815	3.92	4.02	1.4	9.48	1.2	1.01	7.2	280		A 5 V
148184	2921	χ Oph	357.934	20.677	-0.0835	0.0140	-0.0170	4.62	4.13	5.3	4.33	-4.6	1.82	7.1	263	M	B 1.5 V e
148199	3654		349.461	13.475	0.2905	0.0753	0.1004	4.07	4.06	2.1	7.03	-0.0	0.56	6.4	198	m	B 8 V Si
148302	3434		351.737	15.262	0.3550	0.1149	0.1638	3.89	4.24	0.9	10.01	2.2	0.95	6.7	227	m	A 7 V
148321	3355		352.531	15.906	0.3850	0.1020	0.1810	3.92	4.36	0.9	6.99	2.2	0.19	4.5	80		A 5 m p Sr
148334	3435		351.622	15.105	0.3073	0.0584	0.1137	4.06	4.22	1.9	9.95	0.5	0.83	8.5	514		B 9 V
148499	3516		351.092	14.280	0.3718	0.0870	0.1147	4.02	3.72	2.2	9.84	-0.5	1.32	9.0	656		
148562	3270		353.161	15.936	0.4032	0.0990	0.1877	3.96	4.42	1.2	7.84	1.8	0.31	5.7	140	m	A 3 V
148563	3438		351.906	14.872	0.4107	0.0912	0.1834	3.96	4.30	1.2	8.61	1.7	0.53	6.3	185	m	A 2 V
148579	3271		353.040	15.812	0.3180	0.0660	0.1174	4.05	4.20	1.8	7.35	0.5	1.05	5.7	141	m	B 9 V

The chemically peculiar stars were *not* included in the determination of the average distances. In Fig. 9 we see a slight rise in the distance as we go to higher galactic longitudes. A similar effect was found by Jones (1970) who used distances based on the parallaxes of the stars. The spread in distance in Fig. 9 is due to the intrinsic depth structure of the subgroups, combined with the error in the distance determination. A comparison with the study by Jones (1970), who used the latest proper motion data (from the FK 4), shows a good agreement of the averages for the three subgroups. A star-to-star comparison of the distances from Jones's and our study is shown in Fig. 10. Within the errors the two studies give the same result. This implies that the relative proper-motion distances reflect the depth structure of each subgroup, which will become very important for the study of the interaction of the stars with the gas.

The spread in the photometric distances of the member stars is used to define boundaries within which we expect all members to lie. Figure 11 again shows a plot of distance modulus versus galactic longitude, but now for all our programme stars. The lines drawn in are the adopted boundaries of the groups. We see from Fig. 11 that many stars. The lines drawn in are the adopted boundaries of the groups. We see from Fig. 11 that many stars are definitely not members of the association. The membership criterion for each separate star is given in column 17 of Table 3.

5.2. *Upper-Scorpius and the Ophiuchus dark clouds*

The youngest of the three subgroups of Scorpio-Centaurus, Upper-Scorpius, is an extremely interesting object because of its vicinity to the Ophiuchus dark clouds. In this section we will combine properties of the stars in the subgroup with properties of the dark clouds, in order to establish their relationship in a more quantitative way.

All previous photometric studies of Sco OB 2 concluded that the Upper-Scorpius subgroup shows a much higher mean visual extinction than the other two (e.g. Gutierrez-Moreno et al., 1968; Garrison, 1967). Within the Upper-Scorpius subgroup however considerable spread in A_V is also found. In Fig. 12 we plotted the

Table 3c (continued)

HD (1)	Hipp (2)	Name (3)	l ° (4)	b ° (5)	[B − U] (6)	[U − W] (7)	[B − L] (8)	log T_{eff} (9)	log g (10)	log $L/L_{\odot}$ (11)	m_V m (12)	M_V m (13)	A_V m (14)	D.M. m (15)	Dist. pc. (16)	Mem. (17)	MK Spectral Type (18)
148594	3517		350.930	13.939	0.2539	0.0596	0.0829	4.10	3.90	2.5	6.91	-0.7	0.65	6.9	249	M	B 8 V nn
148605	3272	22 Sco	353.100	15.796	0.0890	0.0140	0.0398	4.29	4.26	3.1	4.79	-1.1	0.22	5.7	141	M	B 2 V
148624	3440		352.086	14.905	0.4082	0.1171	0.1816	3.96	4.32	1.2	10.38	1.7	1.13	7.5	321		A 7 IV
148703	3879		345.943	9.218	0.0557	0.0080	0.0246	4.33	4.16	3.5	4.24	-1.9	0.19	5.9	154	M	B 2 III
148822	3443		352.177	14.538	0.3044	0.1095	0.1525	3.88	4.40	0.7	9.65	2.8	0.68	6.1	170	m	F 0 V
148842	3444		352.166	14.493	0.4190	0.1028	0.1724	3.91	3.88	1.5	10.65	0.9	0.36	9.3	727		A 1 V
148860	2897		359.291	20.299	0.3516	0.0811	0.1261	4.03	4.12	1.8	8.04	0.5	0.65	6.8	234	m	B 9.5 V
149069	3445		352.047	13.944	0.4131	0.0896	0.1596	3.98	4.06	1.6	10.50	0.7	0.64	9.0	657		A 1 V
149168	3446		352.597	14.232	0.2216	0.0423	0.0903	4.13	4.36	2.2	9.92	0.3	0.57	9.0	644		B 7 V
149228	3359		353.400	14.794	0.2024	0.0529	0.0721	4.15	4.02	2.6	10.01	-0.7	1.39	9.3	733		B 9 p Si
149367	3447		352.798	14.046	0.3107	0.0692	0.1082	4.06	4.08	2.0	8.53	0.0	0.73	7.7	350		B 9 V
149387	3718		349.893	11.529	0.1958	0.0510	0.0649	4.15	3.86	2.8	9.21	-1.2	0.93	9.5	812		
149438	3519	τ Sco	351.536	12.808	-0.0276	-0.0057	-0.0133	4.47	3.86	4.7	2.82	-4.2	0.11	6.9	247	M	B 0 V
149464	3590		351.449	12.688	0.3513	0.0765	0.1288	4.03	4.16	1.8	8.61	0.6	0.71	7.2	278		B 9 V n
149757	84	ζ Oph	366.282	23.588	-0.0368	0.0055	-0.0187	4.47	3.62	5.0	2.57	-5.1	0.91	6.8	228	M	O 9.5 V n n(e)
149883	3448		352.896	13.145	0.3563	0.0802	0.1240	4.03	4.04	1.9	8.45	0.3	0.60	7.5	318		B 9 V
150035	3521		352.799	12.797	0.4157	0.1191	0.1525	3.98	3.96	1.7	8.69	0.4	0.79	7.4	304		A 5 p Sr Cr
150347	3591		352.079	11.612	0.3448	0.0851	0.1137	4.04	3.96	2.0	8.99	-0.0	0.48	8.5	510		B 9 V
150514	2969		358.906	16.789	0.2765	0.0796	0.0809	4.08	3.68	2.6	8.66	-1.2	0.67	9.2	711		B 8 III
151310	3061		358.059	14.608	0.1018	0.0201	0.0379	4.27	4.00	3.3	9.38	-1.7	0.71	10.4	1230		B 2 V
151346	3196		356.641	13.446	0.1833	0.0562	0.0579	4.16	3.76	3.0	7.93	-1.7	1.73	7.9	390		B 7 V p wk He
151831	3453		354.837	11.159	0.2646	0.0692	0.0864	4.09	3.90	2.4	10.52	-0.6	0.52	10.6	1360		
151865	2975		360.484	15.394	0.2715	0.0665	0.1004	4.09	4.20	2.0	8.85	0.2	0.79	7.7	360		B 8 V
151890	748	μ^1 Sco	346.117	3.914	0.0490	0.0040	0.0162	4.34	3.86	3.9	3.00	-2.9	0.11	5.8	147	M	B 1 V
151985	750	μ^2 Sco	346.198	3.862	0.0420	0.0080	0.0142	4.35	3.90	3.9	3.56	-2.9	0.08	6.4	191	M	B 2 IV
154481	3460		357.243	8.470	0.2964	0.0929	0.0781	4.06	3.46	2.8	6.27	-1.8	0.20	7.9	381		
157056	3303	θ Oph	360.466	6.553	0.0453	0.0094	0.0178	4.35	4.04	3.7	3.26	-2.4	0.09	5.5	130	M	B 2 IV

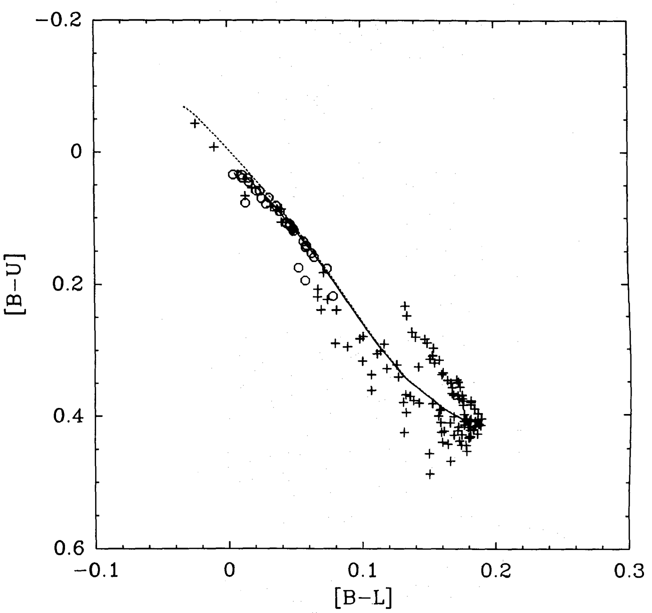

Fig. 7a. As Fig. 6a, for the stars in the Upper-Centaurus Lupus subgroup. The dashed line shows the position of the ZAMS, and the full line indicates the best-fitting isochrone of age 14.5 million years

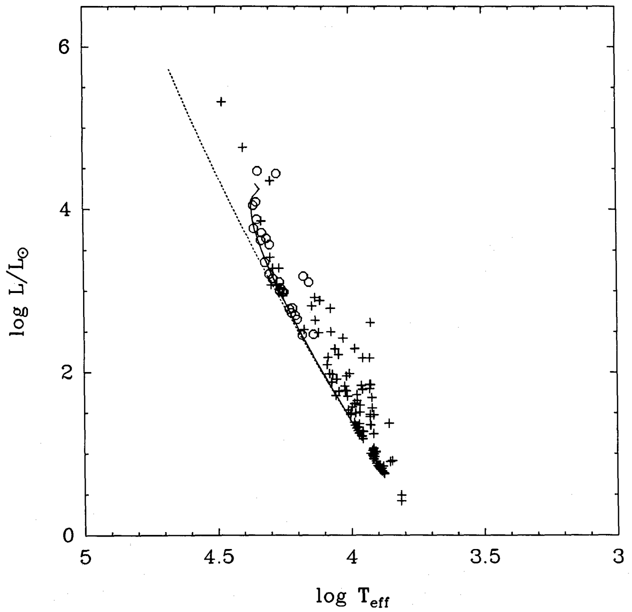

Fig. 7b. As Fig. 6b, for the stars in the Upper-Centaurus Lupus subgroup. The two stars (+) lying at log $L/L_{\odot} > 4.5$ turn out to be non-members. The two lines have the same meaning as in Fig. 7a

stars in Upper-Scorpius in galactic coordinates, and denoted their visual extinction by the symbol size. It is evident from this plot that the distribution of the extinction is not random. A detailed comparison of the IRAS 100 μm map of Fig. 13 with A_V (Fig. 12) shows that there is a tight correlation between the two. From this we conclude that the stars in Upper-Scorpius are located either at the same distance as, or behind the Ophiuchus dark clouds, but definitely not in front of them.

In order to determine the distance to the dark clouds in Ophiuchus we followed the same procedure as e.g. Turner (1986), who determined the distance to L 810. We made a plot of A_V as a function of distance modulus (Fig. 14). The presence of stars at large distance moduli but with low visual extinctions is caused by the fact that the distribution of the dust is extremely irregular see Fig. 13): stars may be behind a region containing little dust. The flattening of the extinction as a function of distance modulus occurs at the far side of the cloud. Stars at a larger distance will have the same extinction. The observations however show a drop at distance moduli larger than 7^m. This drop is due to the completeness limit of our programme. As was pointed out in

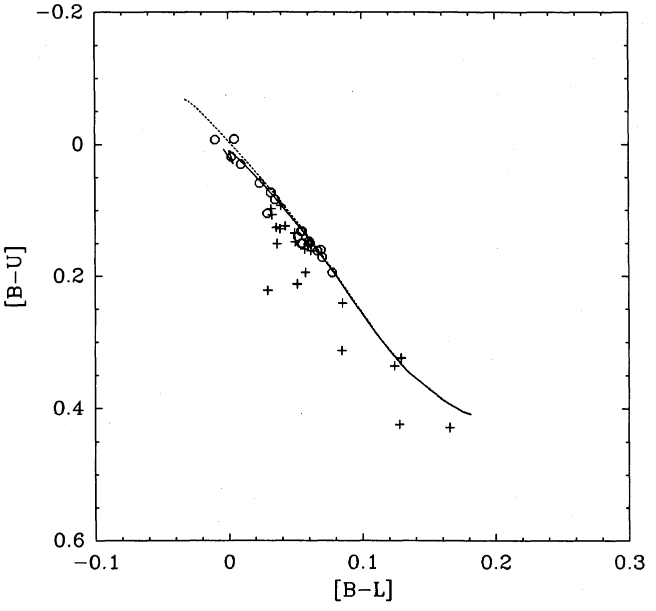

Fig. 8a. As Fig. 7a, for the stars in the Lower-Centaurus Crux subgroup. The dashed line shows the ZAMS, and the full line indicates the position of the isochrone of age 11.5 million years

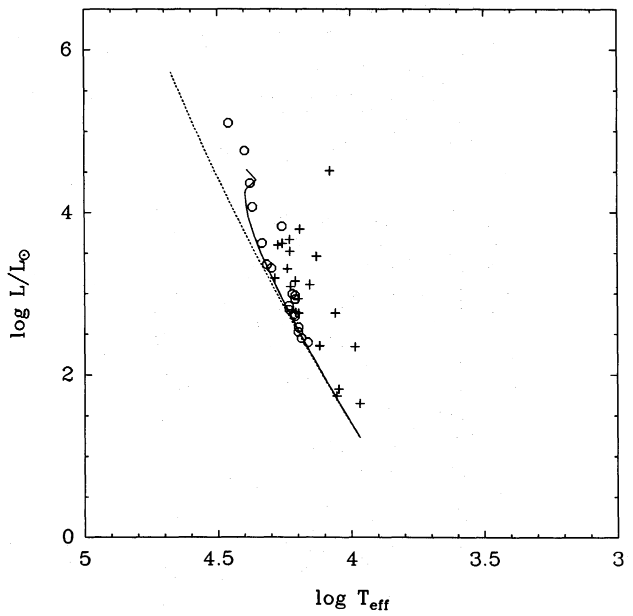

Fig. 8b. As Fig. 7b, for the stars in the Lower-Centaurus Crux subgroup. The member star at log $L/L_{\odot} > 5$ is the emission line star δ Cen. The two lines have the same meaning as in Fig. 8a.

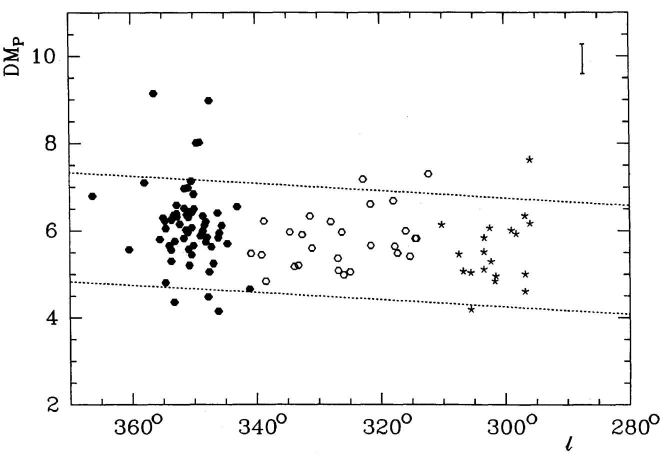

Fig. 9. Distance modulus as a function of galactic longitude for the established member-stars of the three subgroups. ●: Upper-Scorpius; ○: Upper-Centaurus Lupus; ⋆: Lower-Centaurus Crux. The average error in the distance modulus is indicated by the errorbar in the top-right corner. The dashed lines indicate the adopted boundaries of the subgroups. There is a general trend for the distances to be larger towards larger longitudes

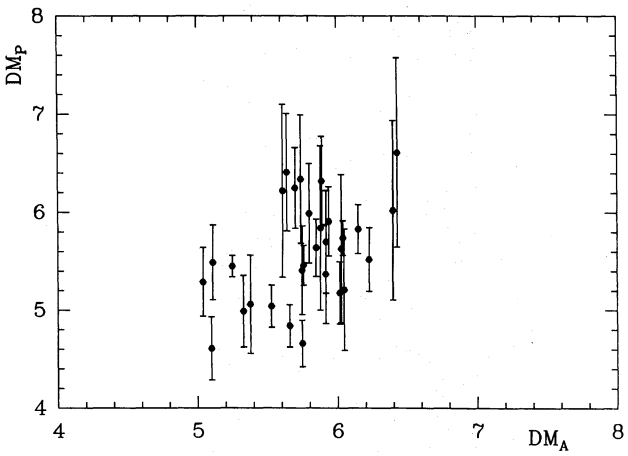

Fig. 10. Distance modulus based on the photometric data plotted against the distance modulus from proper motions (Jones, 1971). From this figure stars with emission-line spectra and chemical peculiarities were excluded

Sect. 2.1 this limit is at roughly 9^{m}. So given a certain spectral type (i.e. M_V), we can translate the completeness limit into terms of A_V and distance modulus. In Fig. 14 the full line shows this limit in case of a B 5 V star. To the right of this line only programme stars of a spectral type earlier than B 5 V are possible, and because of the scarcity of these stars, we see only few.

The most important feature in Fig. 14 is the rise in A_V at small distance moduli. At a certain distance we expect to see the near edge of the cloud, and going towards larger distances we expect A_V to rise, depending on the density-distribution of the dust. At the far edge we expect the plot to flatten again. From this we can determine the distance to, and the depth of, the Ophiuchus dark clouds. This results in the following distance:

$$d\,(\text{near edge}) = 80 \pm 20\,\text{pc},$$
$$d\,(\text{far edge}) = 170 \pm 35\,\text{pc},$$
$$d\,(\text{centre}) = 125 \pm 25\,\text{pc}.$$

The determination of the distance of the dark cloud complex in Ophiuchus with respect to the stars in Upper-Scorpius reveals two very intersting effects: first of all throughout the cloud the stars appear to be evenly distributed in distance, and secondly a number

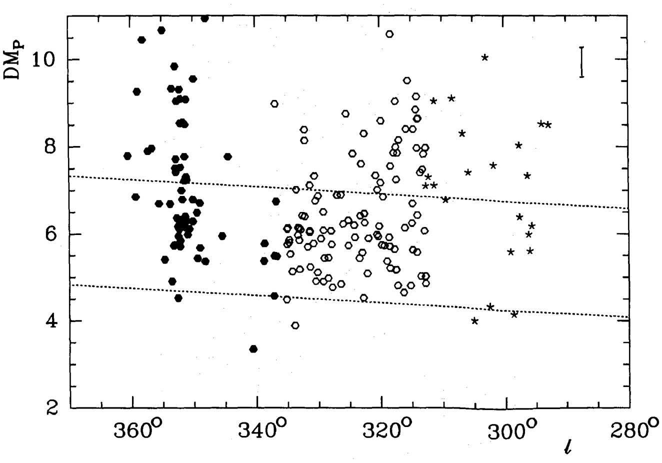

Fig. 11. As Fig. 9, for the remaining stars in the programme. The membership criterion is based on the position of each star in this diagram

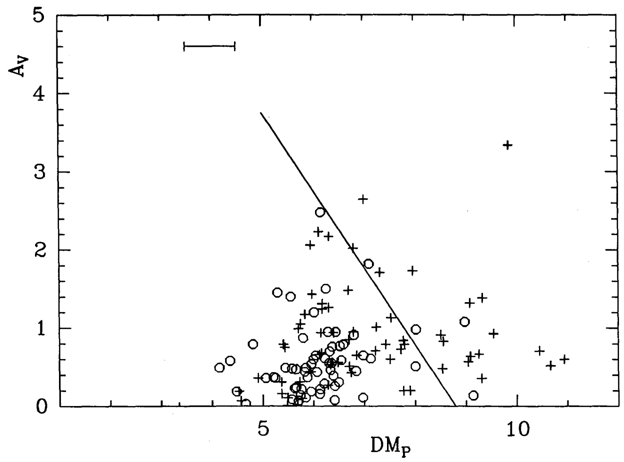

Fig. 14. Plot of the visual extinction as a function of distance modulus for the stars in the Upper-Scorpius region. Circles denote the established members of the subgroup, plusses denotes the remainder of the programme. The line indicates the completeness limit of our sample for B 5 V stars. The rise in visual extinction at distance moduli smaller than 6 shows that a number of stars are distributed throughout the molecular cloud. A number of member stars are indeed found behind the cloud

of stars is actually located *behind* the cloud. These two results will become very important in the detailed study of the interaction processes between the stars and the interstellar medium in this region (de Geus, 1988, in preparation). Straižys (1984) determined the distance to Ophiuchus in a similar way as done here. He derived a distance to the near edge of 120 pc, and argues that the nebula extends up to $d = 200$ pc. We find a smaller distance and, what is more important, that a number of the earliest-type stars lie behind the dark cloud.

6. Conclusions and future work

From the photometric data of 300 stars in the Scorpio-Centaurus OB association we derived several physical properties for its three subgroups. By comparing the HR diagrams for the stars with theoretical isochrones, we obtained nuclear ages. We found somewhat lower ages than de Zeeuw and Brand (1985), due to the use of different models for stellar evolution in the calculation of the isochrones. The classical picture of sequential starformation is clearly not valid for the Sco OB 2 association as a whole, because the oldest subgroup is right inbetween the two younger ones. Possibly, for some unknown reason, massive star formation was ignited near the middle of the giant molecular cloud, forming Upper-Centaurus Lupus, which in turn ignited star-formation in two directions: forming Upper-Scorpius and Lower-Centaurus Crux. The presence of an infrared cluster inside the Upper-Scorpius subgroup (Grasdalen et al., 1973; Vrba et al., 1975; Elias, 1978; Wilking and Lada, 1983) possibly containing early-type stars, indicates a continuing ignition of starformation by the already formed stars.

The distances to the subgroups were found to be a function of galactic longitude, with the Upper-Scorpius subgroup having the largest distance. On the basis of a distance vs. galactic longitude plot of the established member stars we derived the "boundaries" of the association and in this way determined membership for the rest of the stars. This way of membership determination should however be treated with the necessary caution, because of its inaccuracy.

The calculated visual extinctions to the stars in the Upper-Scorpius subgroup were shown to correlate well with the distribution of the dust in the Ophiuchus dark clouds, as seen in the IRAS 100 μm map. From the plot of A_V against distance modulus we found the distance of the Ophiuchus clouds to be: 125 ± 25 pc. The depth of the cloud could also be determined from this plot, the near edge being at 80 ± 20 pc, and the far edge at 170 ± 35 pc. The stars were found to be distributed mainly at the far side of the dark cloud.

The fact that a number of the brightest stars are behind the molecular clouds is important for understanding the morphology of the atomic and molecular gas in this region, as well as for understanding the origin of a slow shock seen in CH and CH^+ absorption towards a number of early-type stars in Upper-Scorpius by Meyers et al. (1985). A discussion of the distribution of the interstellar matter in Ophiuchus will be presented in a future paper (de Geus et al., 1988, in preparation).

OB associations are very important objects for the calibration of the distance scale. The lack of knowledge regarding membership of OB associations and the lack of accurate distances for stars over a large range in spectral types are the two most important problems in the study of these groups. The observations by the HIPPARCOS satellite will be a major improvement on this. The first results are anticipated around 1992/1993. In order to determine the radial velocities of the stars we are obtaining high-resolution spectra of candidate member stars in nearby associations. These radial velocities will already give us a more accurate determination of the membership than based on the photometry.

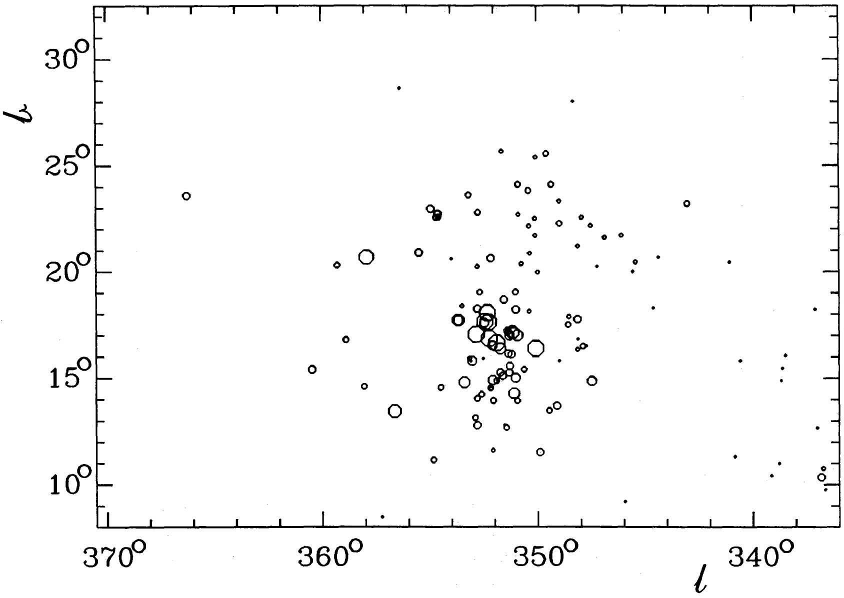

Fig. 12. Map in galactic coordinates of the visual extinction towards the stars in Upper-Scorpius. The size of the symbol denotes the strength of the extinction ($A_{V,\max} = 3\overset{m}{.}5$). Comparison of this figure with Fig. 13 shows that the stars cannot be in front of the Ophiuchus molecular clouds

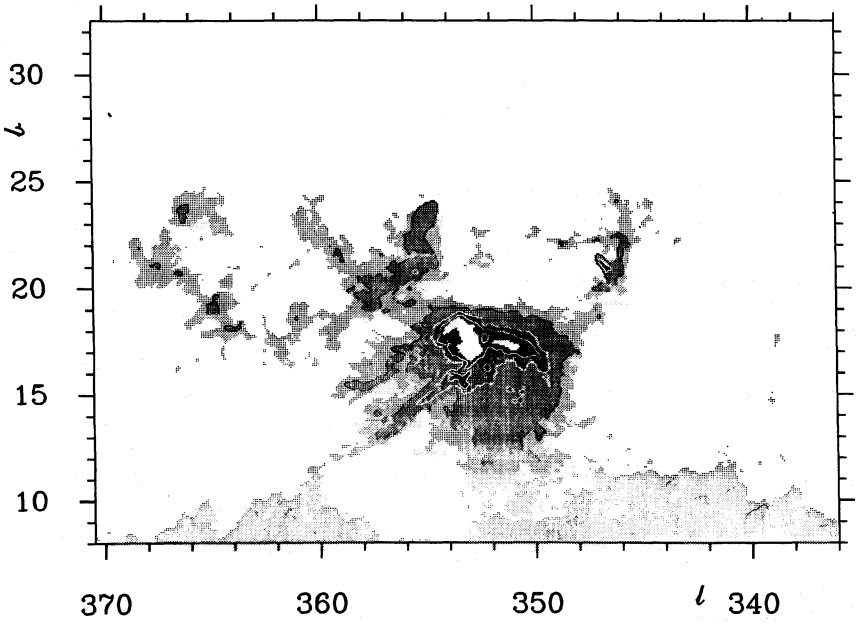

Fig. 13. Map of the IRAS 100 µm emission in the Ophiuchus dark cloud. The emission at 100 µm is a measure of the amount of dust along the line of sight. The fact that the features in this map are closely traced by the values of the extinction of the stars, enables us to estimate the distance to the Ophiuchus molecular cloud

Acknowledgements. It is a pleasure to thank Prof. A. Blaauw for his continued interest, and for constructive criticism on the manuscript. We thank the following students, who have spent cold and lonely weeks on La Silla observing stars for this programme: J.W. de Bruyn, J.H. Burger, J. Hooimeyer, A. Roobeek, P. Houtekamer, and H. Röttgering. TdZ was supported in part by an RCA Fellowship.

References

Barlow, M.J., Cohen, M.: 1977, *Astrophys. J.* **213**, 737
Bertiau, F.C.S.J.: 1958, *Astrophys. J.* **128**, 533
Blaauw, A.: 1946, Ph. D. Thesis, University of Groningen
Blaauw, A.: 1961, *Bull. Astron. Inst. Neth.* **15**, 265
Blaauw, A.: 1964, *Ann. Rev. Astron. Astrophys.* **2**, 213
Blaauw, A.: 1978, in *Problems of Physics and Evolution of the Universe*, ed. L. Mirzoyan, Yerevan, USSR, p. 101
Blaauw, A., Morgan, W.W., Bertiau, F.C.: 1955, *Astrophys. J.* **121** (2)
Brand, J., Wouterloot, J.G.A.: 1988, *Astron. Astrophys. Suppl.* **75**, 117
Buscombe, W.: 1974, *General Catalogue of MK Spectral Classifications*, Vol. 1–5
Collins, G.W., Sonneborn, G.H.: 1977, *Astrophys. J. Suppl.* **34**, 41
Crawford, D.L.: 1978, *Astron. J.* **83**, 48
de Geus, E.J.: 1984, M. Sc. Thesis, University of Leiden
de Ruiter, H., Lub, J.: 1985, *Astron. Astrophys. Suppl.* **63**, 59
de Zeeuw, P.T., Brand, J.: 1985, in *Birth and Evolution of massive stars and stellar groups*, eds. H. van Woerden, W. Boland, Reidel, Dordrecht, p. 95
Elias, J.H.: 1978, *Astrophys. J.* **224**, 453

Elmegreen, B.G., Lada, C.J.: 1977, *Astrophys. J.* **214**, 725
Garrison, R.F.: 1967, *Astrophys. J.* **147**, 1003
Glaspey, J.W.: 1971, *Astron. J.* **76**, (10), 1041
Grasdalen, G.L., Strom, K., Strom, S.E.: 1973, *Astrophys. J.* **184**, L 53
Gutierrez-Moreno, A., Moreno, H.: 1968, *Astrophys. J. Suppl.* **15**, 459
Hackwell, J.A., Gehrz, R.D.: 1974, *Astrophys. J.* **194**, 49
Hardie, R.H., Crawford, D.L.: 1961, *Astrophys. J.* **133**, 843
Harris, D.H.: 1973, in *IAU Symposium* **52**, *Interstellar Dust and Related Topics*, eds. J.M. Greenberg, H.C. van de Hulst, Reidel, Dordrecht, p. 31
Hauck, B., Mermilliod, M.: 1980, *Astron. Astrophys. Suppl.* **40**, 1
Jones, D.H.P.: 1970, *Monthly Notices Roy. Astron. Soc.* **152**, 231
Jung, J., Bischoff, M.: 1971, *Bulletin d'Information du Centre de Donnees Stellaires* **2**, 8
Kurucz, R.: 1979, *Astrophys. J. Suppl.* **40**, 1
Larson, R.: 1986, *Monthly Notices Roy. Astron. Soc.* **218**, 409
Lub, J.: 1979, *The Messenger* **19**, 1
Lub, J., Pel, J.W.: 1977, *Astron. Astrophys.* **54**, 137
Maeder, A.: 1981a, *Astron. Astrophys.* **93**, 136
Maeder, A.: 1981b, *Astron. Astrophys.* **99**, 97
Maeder, A.: 1981c, *Astron. Astrophys.* **102**, 401
Mathieu, R.D.: 1986, *Highlights of Astronomy* **7**, 481
Meyers, K.A., Snow, T.P., Federman, S.R., Breger, M.: 1985, *Astrophys. J.* **288**, 148
Schultz, G.V., Weimar, W.: 1975, *Astron. Astrophys.* **43**, 133
Sneden, C., Gehrz, R.D., Hackwell, J.A., York, D.G., Snow, T.P.: 1978, *Astrophys. J.* **223**, 168
Straižys, V.: 1984, *Vilniaus Astron. Obs. Biul.* **67**, 3
Straižys, V., Kuriliene, G.: 1981, *Astrophys. Sp. Sci.* **80**, 353
Turner, D.G.: 1986, *Astron. Astrophys.* **167**, 157
Vrba, F.J., Strom, K.M., Strom, S.E., Grasdalen, G.L.: 1975, *Astrophys. J.* **197**, 77
Whittet, D.C.B.: 1974, *Monthly Notices Roy. Astron. Soc.* **168**, 371
Wilking, B.A., Lada, C.J.: 1983, *Astrophys. J.* **274**, 698